Synthesis of low co-ordinate heteroleptic first row transition metal complexes.

Olivia Churchill, BA (Hons)

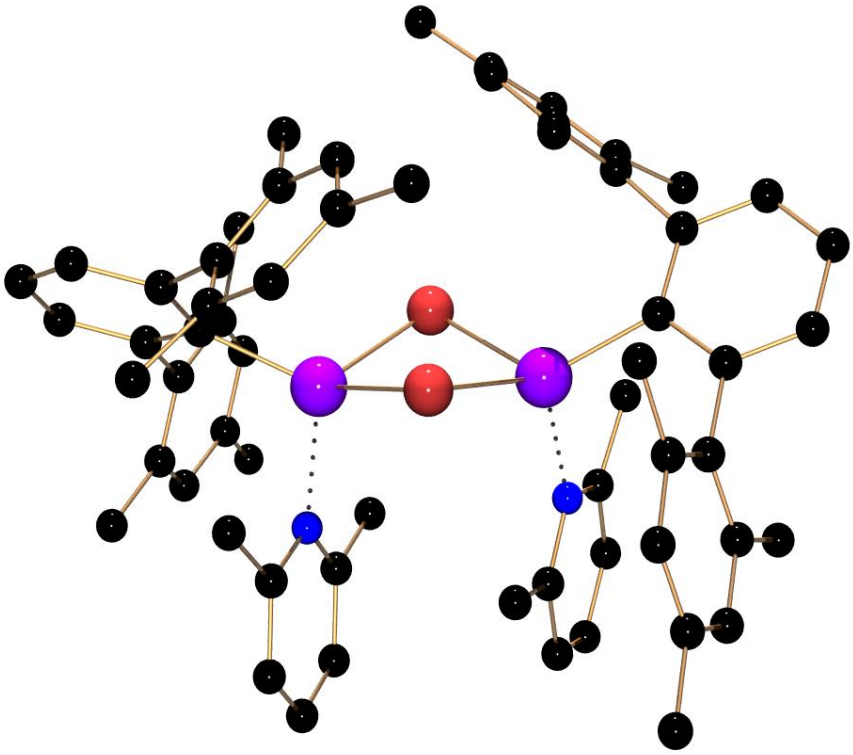

Thesis submitted to the University of Nottingham for the degree the degree of Master of Research in Chemistry

September 2018

Declaration

The work described in this thesis was carried out at the University of Nottingham in the laboratory B46 between October 2017 and September 2018, under the supervision of Dr Deborah L. Kays. All the work is my own unless otherwise stated and has not been previously submitted for any degrees at this or any other university.

Olivia Churchill

Abstract:

Low co-ordinate transition metal complexes have attracted much interest in recent years due to their high reactivity and unusual magnetic properties. These complexes have often been achieved with the use of bulky *m*-terphenyl ligands, which have enabled the formation of monomeric and dimeric transition metal complexes. They have also enabled the stabilisation of novel species with unusual bonding modes and oxidation states.

The synthesis of a new cyclic alkyl amino carbene (CAACs) has been attempted. These ligands, developed after the heavily investigated and versatile carbenes, N-heterocyclic carbenes (NHCs), differ by the presence of a quaternary carbon in place of a nitrogen, resulting in a smaller HOMO/LUMO separation. This is significant as it means that CAACs are more nucleophilic (σ-donating) and more electrophilic (π accepting), both properties that can be exploited within transition metal complexes. The increased electrophilic character of the CAAC makes it a poor leaving group, providing a good framework for a catalyst. These properties therefore make the synthesis of a new CAAC ligand potentially able to stabilise a low co-ordinate metal centre a promising area to explore.

The synthesis of a selection of metal halide-bridged dimers $[Mes_2C_6H_3MX]_2.[LiX(OEt_2)]_2$ (where M= Mn, Fe, Co, Zn and X = Cl, Br) was carried out with the previously synthesised $[2,6\text{-}Mes_2C_6H_3Li]_2$. These were then

used as precursors, with the addition of a monodentate pyridine-based ligand to give a selection of novel three and four co-ordinate complexes of the general formula $[Mes_2C_6H_3MBr(2,6\text{-}MesC_5H_3N)]_2$ and $[Mes_2C_6H_3MCl(2,6\text{-}MesC_5H_3N)]$. Steps were taken for the initial characterisation of the complexes, with the use of NMR spectroscopy, X-ray diffraction measurements and Evans NMR spectroscopy.

Acknowledgements

First and foremost, I would like to thank my supervisor, Dr Debbie Kays for her support and understanding, both academically and personally throughout my project.

I would also like to thank the members of the Kays groups for making me feel welcome and Supported. To Gareth and Ana for their patience and guidance in teaching me how to work in the lab, as well as their enthusiasm and encouragement. To Andy, Rob, Charlotte and Laurence for all your help and making me laugh and to Amy, Glenn and Yu, for making the lab and office a lovely place to be.

I would like to thank Dr William Lewis and Prof Sandy Blake for training and teaching me about X-ray diffraction. Mr Shazam Aslam and Dr Kevin Butler for NMR training and help with NMR spectroscopy.

To my Aunt and Uncle for their endless care and help. To Sarah, Immie, Freya and James (last but in no ways least) for your unconditional love and support.

List of Abbreviations

Ar	Any aromatic group
Dipp	2,6-Diisopropylphenyl, 2,6-$^{i}Pr_2C_6H_3^-$
^{i}Pr	Isopropyl (Me_2CH^-)
Me	Methyl (CH_3^-)
Mes	Mesityl, 2,4,6- trimethylphenyl, 2,4,6-$Me_3C_6H_2^-$
Np	2,2-Dimethyl propane
THF	Tetrahydrofuran (C_4H_8O)
^{t}Bu	tert-Butyl (Me_3C^-)
^{n}Bu	Normal Butyl ($CH_3CH_2CH_2CH_2^-$)
Ph	Phenyl, $C_6H_5^-$
R	Alkyl group
RT	Room temperature
LDA	Lithium diisopropylamide
XRD	X-Ray diffraction

s	Singlet
d	Doublet
t	Triplet
br	Broad

Table of Contents

1. Introduction

1.1 Organometallic Compounds

Organometallic compounds are those that are defined by a metal-carbon bonding interaction and have been explored since the early 1800s. Conventional ligands of the time containing oxygen, nitrogen or phosphorus typically bond through a lone pair that can act in a dative manner and donate to the metal centre. These complexes where the metal centre binds to a non-carbon ligand are called Werner complexes (Figure 1). Carbon traditionally lacks a lone pair of electrons that can do this, so M-C bonds are usually σ or π bonding. Before 1970 compared with two decades prior, examples of transition metal complexes with metal-carbon bonds were few and tended to contain ligands such as CO, alkenes, pyridine and cyclopentadienyl. These ligands all have π systems which are available to act as π acceptors strengthening the bond produced.[1,2]

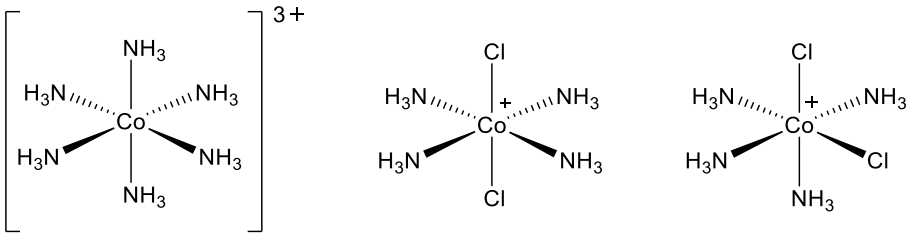

Figure 1. Left is a classic Werner complex, while middle and right contain the trans and cis isomers of $[Co(NH_3)_4Cl_2]^+$, of which Werner synthesised cis isomer for the first time.[2]

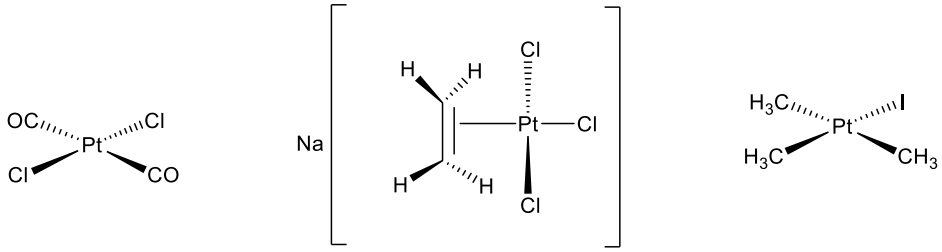

Figure 2. Early examples of transition metal complexes synthesised containing examples of π acceptor ligands and the first σ organo-transition metal complex.[3–5]

Zeise's salt $Na[PtCl_3C_2H_4]$ was the first olefin complex, while $Pt(CO)_2Cl_2$ was the first metal-carbonyl complex to be synthesised in 1827 and 1868 respectively (Figure 2).[4,5] These complexes contain ligands with π and π* orbital systems capable of stabilising a metal centre. On the far right, $PtI(CH_3)_3$ was synthesised in 1909 and differs from the previous examples, as it is a σ bonded complex containing no π interactions (Figure 2).[3]

Failure in the early 1900s to produce a stable structure containing an M-C alkyl with a transition metal led to the belief that such M-C bonds were weak (particularly with chromium, rhodium and iron).[6] This is not the case as M-C bonds have energies in the range of 30-60 kcal mol^{-1} [7](the exact value depends on the nature of the other substituents, though cobalt has been the subject of many studies giving values ranging from 18-25 kcal mol^{-1}, while manganese gives values from 29-49 kcal mol^{-1}),[8] and it is the existence of facile decomposition pathways that leads to the complexes being kinetically

unstable.[9] This instability is key in processes such a catalysis,[8] as alkyl feedstocks need to bind to the metal strongly enough to react, but not too strongly as to be bound indefinitely and therefore poison the catalyst.

Decomposition routes of kinetically unstable alkyl complexes include β-elimination and reductive elimination, where the former is the major pathway.[10] β-elimination (Scheme 1) can occur whenever the β carbon of the alkyl substituent contains a hydrogen and this is close to the metal centre. The metal centre must also have a vacant site available for co-ordination. With these factors in mind, it is somewhat more apparent why isolation of alkyl based transition metal complexes was limited until appropriate alkyls not featuring β-hydrogen atoms were developed.[11,12]

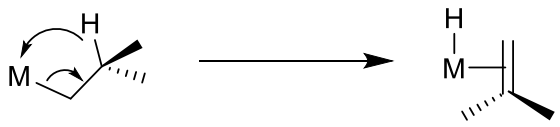

Scheme 1. β-Elimination leading to the formation of a transition metal species containing an alkene and a hydride.

Ligands without a β-hydrogen present for elimination and those with steric bulk are the most likely to produce stable complexes containing M-C alkyl bonds where the metal is a transition metal (examples of stable complexes with M-C alkyl bonds include $Mn[C(SiMe_3)_3]_{2,}$, shown in Scheme 2, and those in Figure 3)[13–16].

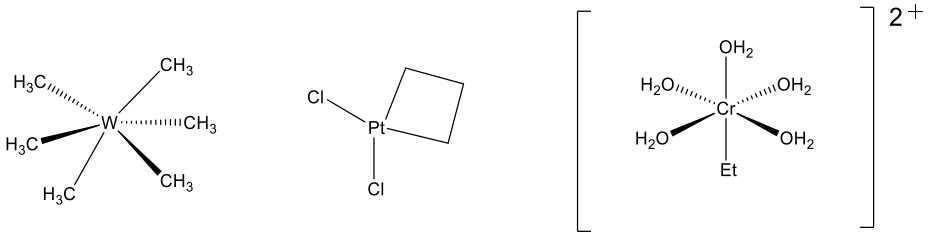

Figure 3. Examples of stable alkyl containing complexes.[13–16]

Many conventional organometallic compounds follow the "18 electron rule" which follows a model assuming molecular orbital overlap between σ and π/π* ligand orbitals of the correct symmetry with the metal d_σ and d_π orbitals. This rule is dependent on the ligand and metal used (as well as the geometry of the system adopted), so is not always applicable to be able to explain the stability of the resultant complexes. Consideration of these individual factors is a much more reliable indication of the stability of a complex, rather than application of the specific "18 electron rule".[1]

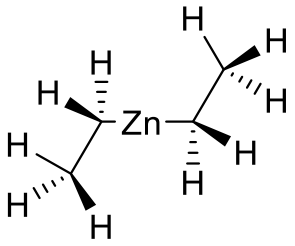

Figure 4. The structure of diethyl zinc

Organozinc compounds were among the first of the organometallic compounds to have been prepared, with the discovery of diethyl zinc in 1848[17] (with the structure confirmed with the use of X-ray diffraction in 2011).[18] This linear low

co-ordinate species (shown in Figure 4) is highly reactive to both air and moisture (due to a high degree of unsaturation and vacant co-ordination sites) and has proved to have several uses within organic synthesis (such as asymmetric addition to imines, Negishi coupling and allylation).[12,19,20] In 1900 the discovery of organomagnesium reagents by Victor Grignard (which would result in the Nobel Prize in Chemistry in 1912) led to a general replacement of the use of these organozinc compounds in synthetic organic chemistry due to ease of use.[21] These species had and continue to have a large impact in the advancement of organic chemistry in synthesis.

Early transition metal organometallic compounds had a larger impact on the theory within inorganic chemistry. These early species including ferrocene, the Ziegler-Natta catalyst and metallocene catalysts (shown in Figure 5, and are representative of the types of complexes synthesised after the discovery of ferrocene.),[22] demonstrated the ability of transition metal-based species to act as catalysts and provide greater understanding of the theory/underlying principles.

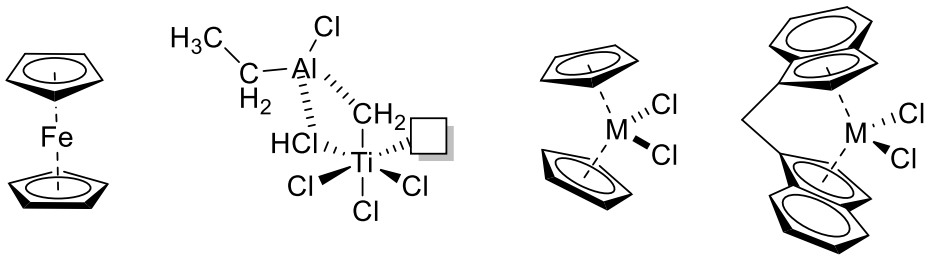

Figure 5. The structures of Ferrocene, the Ziegler-Natta catalyst and two general examples of metallocene catalysts. M= Ti, Zr, Hf[22]

From 1973 to as recently as 2010, the Nobel prize has been awarded within organometallic chemistry to Wilkinson and Fischer (sandwich compounds),[23,24] Grubbs,[25] Schrock[26] and Chauvin[27] (alkene metathesis) and Heck,[28] Negishi[29] and Suzuki[30] (for Pd cross coupling reactions). Many of these discoveries exploit the reactive nature of the metal centres towards alkyl fragments, whilst the structure elucidation of "sandwich compounds" allowed for development of new ideas in organometallic chemistry such as hapticity. Hapticity is the concept in which ligands that contain conjugated or aromatic systems (such as cyclopentadienyl or benzene for example) can donate varying numbers of electrons to the metal centre to stabilise the overall complex.

Metallocene catalysts were developed by Kaminsky (where M= Ti, Zr, Hf).[22] Both the Ziegler-Natta and Kaminsky catalysts are used in alkene polymerisation, with the metallocene catalysts enabling stereospecific control over the polymers produced due to the symmetry of the supporting ligands used.

1.1.2 Low co-ordinate transition metals

Transition metal complexes typically exhibit co-ordination numbers of 4 or above, with any co-ordinations below this number being classed as low co-ordinate. These species are generally air and moisture sensitive making the synthesis challenging, but the resultant species are significant for their properties and geometries. The first example of an open shell two co-ordinate d-block organometallic species was isolated in 1985 by Buttrus, Eaborn and co-workers and is displayed in Scheme 2.[31] The complex is significant as both because of its unusually low co-ordination successfully achieved, as well as the linear geometry (the Mn-C bond lengths are 2.102(4) Å, while the C-Mn-C bond angle is 180°). LiCl is produced as a by-product and acts as an entropic driving factor for the Mn species formation. The large bulky nature of the $C(SiMe_3)_3$ groups, as well as the interlocking positioning leads to the formation of a steric pocket around the Mn which prevents further co-ordination.

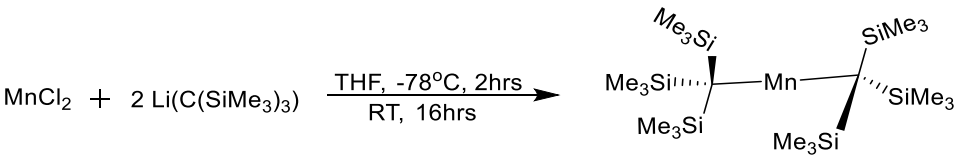

Scheme 2. Reaction scheme for the synthesis of $Mn[C(SiMe_3)_2]_2$.[31]

Early examples of large ligands used to isolate monomeric two co-ordinate complexes include $N(SiMe_3)_2^-$, $CH(SiMe_3)_2^-$ and bulky phosphines (these include

PPh_3 and $P(^{t}Bu)_3$). Typically, alkyl- and aryl-based ligands have been considered less effective at stabilising transition metal centres due to energetically favourable pathways leading to β-elimination and reductive coupling of the alkyl ligands.

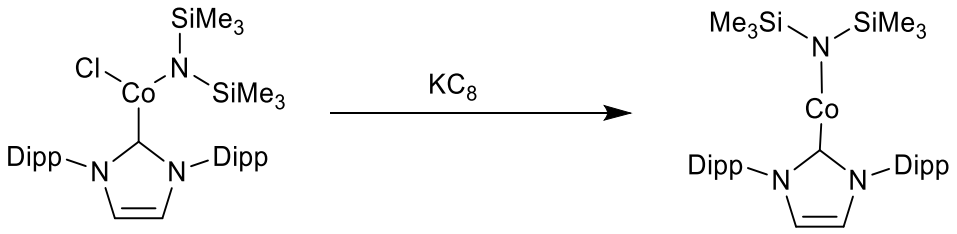

Scheme 3. Example of a reduction used to achieve a low co-ordinate transition metal centre.[32]

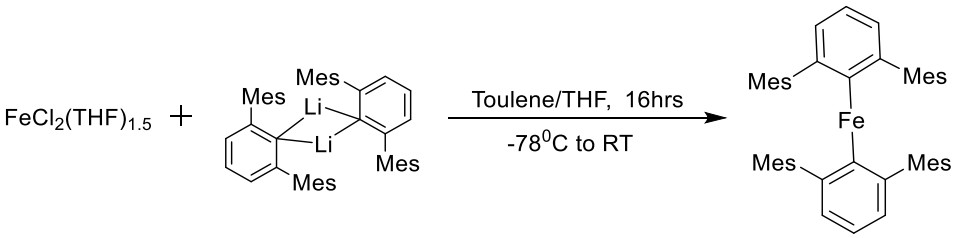

Scheme 4. Salt metathesis reaction of $FeCl_2(THF)_{1.5}$ with one equivalent of lithium salt dimer leading to the two co-ordinate complex.[33,34]

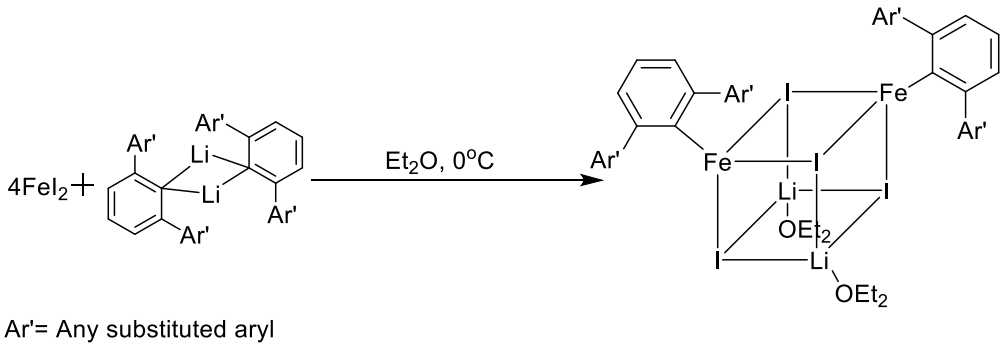

Scheme 5. Salt metathesis reaction of two equivalents of FeI_2 with lithium salt leading to a distinctive cubane structure.[35]

Synthesis of these species can be achieved by a variety of methods but the most common of these are the reduction of organic metal halide precursors (Scheme 3)[32] and a salt metathesis reaction (Scheme 4 and Scheme 5).[33–35] By variation of the ratio of metal halide to lithium salts, a reasonable amount of control can be exerted over the co-ordination of the final product, if not the exact geometry obtained[36]. Although two co-ordinate species are ideally linear, the ligand-M-ligand angle in complexes such as those featuring *m*-terphenyl ligands, is rarely 180° and often deviates.[37–41] This deviation is caused by a range of effects, some of which may result from crystal formation (packing effects) and others which may be a consequence of ligand (secondary interactions within the structure, hybridisation or ligand field effects). Renner-Teller effects can also lead to coupling of excited and ground states with different geometries, which can result in a lowering of energy of a bent configuration.

These considerations can be somewhat neglected in the case of sufficiently sterically bulky ligands, which can help to promote a linear structure. Van der Waals forces also have an impact on the resultant structure regardless of ligand size.

Sterically demanding ligands can facilitate the formation of monomeric complexes but does not guarantee that dimeric or larger structures cannot form. Bulky ligands have helped achieve significant understanding of metal-

metal interactions as well as metal-ligand ones. For example, in 2005, Power and co-workers used an *m*-terphenyl ligand (2,6-$Dipp_2C_6H_3^-$) to isolate the first complex to feature a metal-metal quintuple bonding interaction.[42,43] Use of a bulky ligand was vital in isolating the complex featuring the Cr-Cr multiple bond for several reasons. Large monodentate ligands lead to complexes with low co-ordination due to steric hindrance, which maximises the number of orbitals available to bond with another metal centre whilst reducing the chance of polymerisation (an example of a structure where the use of a smaller ligand results in polymer structure is seen in Figure 7)[44] leading to an increased likelihood of multiple metal-metal bonds (Figure 6).[45]

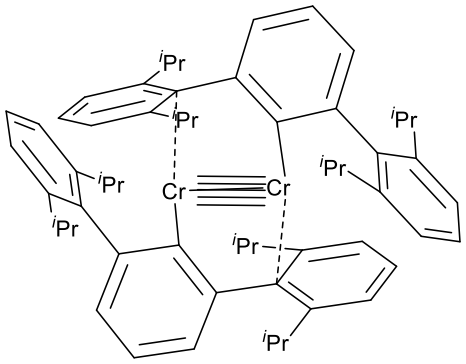

Figure 6. Structure of the first example of a quintuple M-M bond.[42]

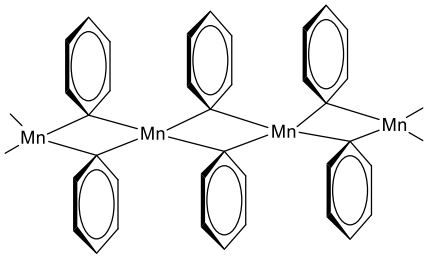

Figure 7. Example of polymeric structure achieved with the use of a less bulky ligand to give $[MnPh_2]_\infty$.[44]

1.1.3 *m*-Terphenyl Ligands

m- Terphenyl ligands are those that have aryl substitutions positioned *meta* to the central bonding carbon, as is shown in the general structure in Figure 8. They are highly tuneable, with a whole range of R_1 groups available to influence the steric pocket created by the flanking aryls with a variety of R_2 such as Me and CF_3 allowing the manipulation of the electronic properties.[46] The positioning of the R_1 groups leads to the formation of the "steric pocket" which shields the metal from further co-ordination, which is the characteristic feature of these ligands, whereas R_2 substitution is thought to allow for greater control over electronic properties[34]. Incorporation of "buttressing" ^{i}Pr substituents at the 3 and 5 positions of the central aryl ring increases the steric demands of the ligand further still.[47,48]

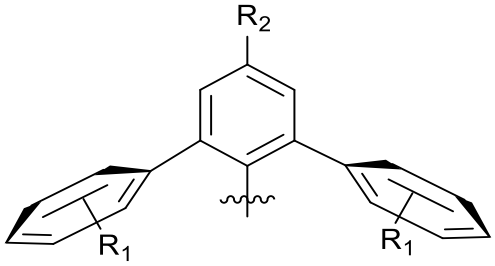

Figure 8. Generalised structure of an m-terphenyl ligand, R_1 and R_2 can be a variety of alkyl or aryl groups.

The central bonding carbon has a sigma bonding interaction with the metal centre and the large flanking groups in the *ortho* positions allow for shielding of a highly reactive open shell metal centre.

This results in a highly reactive metal centre, especially to small molecules as the complex is electronically and co-ordinately unsaturated. The presence of substituents R_1 also serves a secondary purpose of providing a stable aryl that cannot undergo β-hydride elimination.

Synthesis of *m*-terphenyl compounds is relatively simple and involves reacting two equivalents of an aryl Grignard reagent with a lithium 2,6-dihalo aryl complex, followed by quenching with a halogen to give the desired *m*-terphenyl halide (Scheme 6). This reaction is thought to proceed through sequential generation and capture of the benzyne intermediates and the halogenated *m*-terphenyl can be easily converted to the relevant lithium terphenyl for salt metathesis reactions used to form transition metal diaryl complexes. The main synthesis used today was developed in 1996 by Saednya and Hart[49].

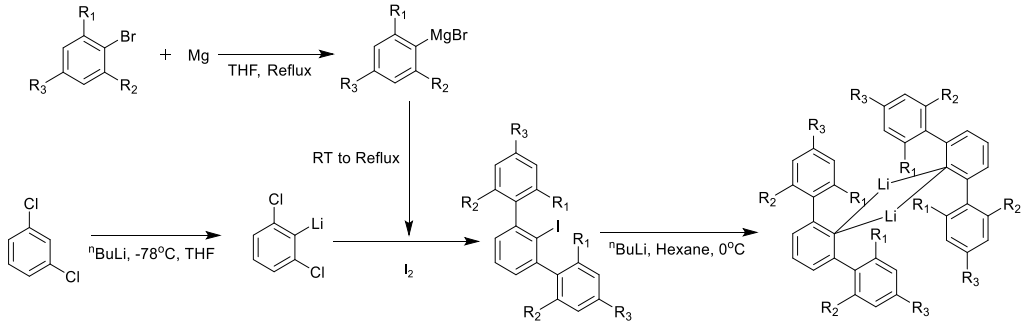

Scheme 6. General synthesis of m-terphenyl ligand. The para position on the main ring is also able to be substituted, and this leads to changing the electronic properties of the ligand once co-ordinated. R_1, R_2 and R_3 are usually alkyl based substituents. [50]

In terms of open-shell complexes, *m*-terphenyl ligands were first used by Power and Ellison in 1996 to isolate the isostructural cobalt and magnesium bromide-bridged dimers with the general formula ($[BrMC_6H_3\text{-}2,6\text{-}Mes_2(THF)_2]$)[51], which have been significant as the first examples of precursors compounds towards species with interesting metal-ligand bonds as well as metal-metal bonds. More recently, methods of creating pure homoleptic species have been developed, giving complexes of the form $[ML_2]$, where M is manganese, iron or cobalt.

Figure 9. Examples of two co-ordinate Mn, Fe and Co complexes.[36,38,39,41,52]

The complexes in Figure 9 have been explored due to their potential magnetic properties and in both stoichiometric and catalytic small molecule investigation, given their high reactivities[52]. This reactivity has been investigated for **(1)** with small molecules including NH_3, O_2, CO and N_2O. This leads to a variety of complexes with interesting geometry (the Fe complex reaction with O_2 yields a rare linear O-Fe-O complex[52] as shown in Figure 10).[41] While Kays and co-workers have investigated **(2)** with a range of reagents,

showing them to behave as pre-catalysts, able to promote dehydrocoupling of dimethylamine-borane[38] and the cyclotrimerisation of isocyanates.[39] (These precatalysts have demonstrated high selectivity not commonly seen within other catalysts used for these reactions.[39,53] Complex **(2)** (where the metal is Fe) is the first example of a transition metal species able to act as pre-catalyst the hydrophosphination of isocyanates, coupled with the ability to produce novel diinsertion products (it is much more common for a mono or poly-insertion product to be favoured).[54] The product distribution is heavily controlled by the reactivity of the substituents, where in most cases either the starting materials are more reactive than the monoinsertion product, (resulting in a majority of monoinsertion product) or where the monoinsertion product is just as reactive as the starting materials (leading to the formation of a polyinsertion/ polymer style product).[55] These diinsertion products are significant as they potentially represent a new family of phosphinodicarboxamides, with exciting properties that could have applications in enantioselective catalysis and co-ordination chemistry.[56]

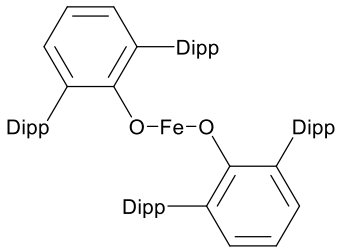

Figure 10. Rare example of a complex containing a linear O-Fe-O unit.[41]

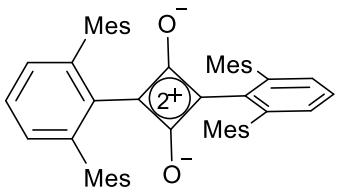

*Figure 11. Squaraine structure produced from reaction of **(2)** with CO.*[37]

CO reactivity has been extensively studied with regards to low co-ordinate *m*-terphenyl systems. The system shown in **(2)** (where the metal is iron in Figure 9) demonstrates the ability to cleave CO bonds (an ability previously unseen for a low co-ordinate iron structure)[57,58] as well as the formation of a squaraine structure (Figure 11), of unusual nature (the level of the delocalisation within the ring appears to be limited due to steric demands of the flanking aryl groups).[37]

1.1.4 Homoleptic and heteroleptic species

Homoleptic complexes contain all the same type of ligand, whereas heteroleptic complexes contain two or more different ligands (specific examples can be seen in Figure 12).[36,59] Within low co-ordinate chemistry the number of homoleptic species is far larger than the heteroleptic variety. Heterolepic species are therefore interesting for their potential implications on both reactivity and magnetism. Single molecular magnets (SMMs) in some examples have shown higher effective barriers and blocking temperatures for

heteroleptic complexes than their homoleptic counterparts.[60] This is significant as many applications (ultrahigh-density information storage devices in particular) require higher blocking temperatures (where blocking temperature is the temperature below which magnetic relaxation becomes slow in comparison to the time scale of the investigation technique).[61]

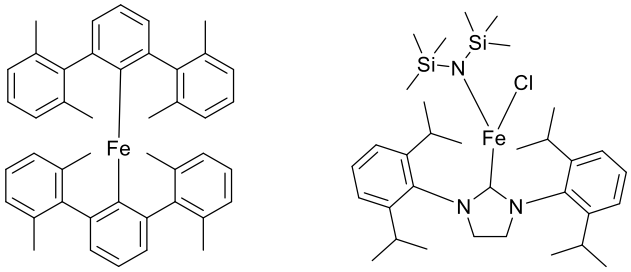

Figure 12. Example of a homoleptic (left) and heteroleptic complex (right). [36,59]

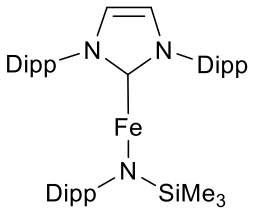

Figure 13. The first example of heteroleptic two co-ordinate Fe complex.[62]

The complex in Figure 13 is the first example of a heteroleptic two co-ordinate iron complex. It has also been explored as a catalyst for the cyclotrimerization of terminal or internal alkynes, proving to be a competent catalyst under moderate loadings in mild conditions.[62]

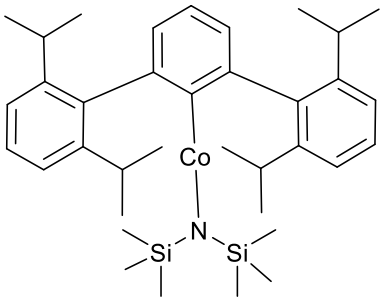

Figure 14. A two co-ordinate Co complex with interesting magnetic properties.[63]

Figure 14 shows the first reported heteroleptic linear two co-ordinate Co complex (C-Co-N bond angle is 179.02(11)°). The complex displays an unexpected large magnetic moment of 5.65 μ_B and obeys the Curie-Weiss law (the Curie-Weiss law is shown in the first equation below) between 2 and 170 K.[63] The Curie constant for a metal complex gives information that can then be used to determine the magnetic moment, and predict the number of unpaired electrons in the system (note that the equation shown below is approximate for the spin only contribution, as this does not take into account spin orbit coupling and orbit effects).

$$x_m = \frac{C}{(T + \theta)}$$

$$x_m = Magnetic\ susceptibilty\ , \qquad C = Curie\ constant,$$

$$\theta = Weiss\ constant, \qquad T = Temperature$$

$$\mu_{eff} = 2.34\sqrt{C} \approx g\sqrt{S(S+1)}$$

$$\mu_{eff} = Effective\ magnetic\ moment, \qquad C = Curie\ constant,$$

$$g = Gyromagnetic\ ratio\ for\ a\ free\ electron,$$

$$S = number\ of\ unpaired\ electrons$$

1.2 Carbenes

Carbenes were first mentioned within the literature with regards to metal centres from 1964 with the characterisation of $W(CO)_5(OCH_3)(CH_3)$.[64] Carbenes can be considered as sp^2 hybridised carbon centres with the ability to form a "double bond" with a metal centre as shown in Figure 15 and are defined as divalent carbon centres.[65–67] R_1 and R_2 are not limited to protons but can be other main group elements (carbon and nitrogen being common examples).

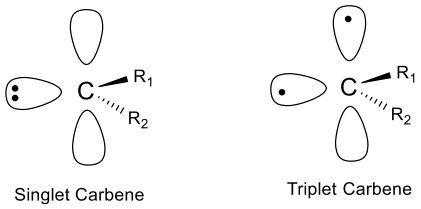

Figure 15. Structure of a singlet and triplet carbene. These are distinct spin isomers with R_1-C-R_2 angles and not resonant structures that exist in an equilibrium.

Carbenes are generally both kinetically and thermodynamically unstable as free ligands and therefore tend to bind strongly to metal atoms. The triplet carbene state is lower in energy to the singlet state as the energy associated with paired electrons in a p orbital is higher than the energy of the two separate electrons in the p and sp hybridised orbitals. These carbenes are known more commonly

as Fischer and Schrock carbenes (Figure 15). Real examples of carbene complexes do not always fit conveniently into these categories and can display characteristics somewhere between these two extremes (Figure 16).[68,69] It is also worth noting that the term "carbene" can imply that the ligand acts as a neutral donor and does not have to change the oxidation state of the metal on co-ordination.

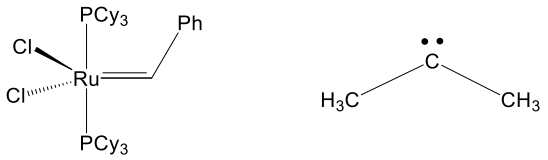

Figure 16. Grubbs 1st generation catalyst (left), which displays some barrier to rotation around the double bond (more than would be expected for a typical Fischer type) but less than would be expected of a Schrock type.[68] *Dimethylcarbene has a ≈1.4 kcal mol-1 energy separation between the triplet and singlet configurations.*[69]

Triplet and singlet carbenes display different types of reactivity and geometry (Figure 17).[70] Singlet carbenes are generally known as Fischer carbenes and can be considered to have a sp^2 hybridisation with a "lone pair" of electrons in an sp^2 hybridised orbital within the plane, while the p orbital is unoccupied. Fischer carbenes are electrophilic at the carbon centre and prone to nucleophilic attack. Triplet carbenes are generally known as Schrock carbenes and are nucleophilic at the carbon centre (Table 1). Both Fischer and Schrock carbenes prefer to adopt bent geometries.

Figure 17. Examples of carbenes with calculated angles and separation energy for the singlet and triplet states. Left (2.94 kcal mol^{-1}. 119.5° for singlet state, 142.88° for the triplet state), Right (2.75 kcal mol^{-1}. 106.96° for singlet state, 135.67° for the triplet state).[70]

Property	**Fischer**	**Schrock**
Nature of carbene carbon	Electrophilic	Nucleophilic
Typical R groups	π Donor (e.g. -OR)	Alkyl, H
Typical metals	Mo(0), Fe(0)	Ta(V), W(VI)
Typical ligands	Good π acceptors (e.g. CO)	Cl, Cp, Alkyl
Electron count (covalent method)	2e(L)	2e(X_2)
Electron count (ionic model)	2e	4e
Oxidation state change on addition of CR_2 to L_nM	0	+2

Table 1. Table from Crabtree's The organometallic chemistry of the transition metals highlighting the key difference between Fischer and Schrock type carbenes.[2]

1.2.1 Schrock Carbenes

Schrock carbenes are defined by their triplet state and typically have a geometry that is bent but more similar to a linear, or unhybridized state than Fischer carbenes. In the 1970s during an attempted synthesis of a "tantalum ylide" (an analogue of the phosphorus ylide) the first Schrock carbene (co-ordinated to a metal centre) was created.[71] The carbene acts in a nucleophilic manner and through consideration of the bond lengths of Ta-CH_3 (2.25 Å) with Ta=CH_2 (2.02 Å) indicated that there was a Ta=C double bond. Early complexes containing Schrock carbenes rarely meet the 18 electron rule (Figure 19).[72] These high oxidation state complexes, typically with early transition metals also contain ligands able to provide additional stabilisation. This includes ligands such as halides with lone pairs capable of donating into the d orbitals and alkyls which have C-H bonds which can become agostic (as shown in Figure 18, in which one hydrogen attached to a carbon centre also co-ordinates to the metal centre), which increases the electron density on the metal centre leading to stabilisation of the complex.[73]

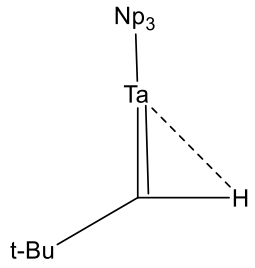

Figure 18. Example of an agostic interaction of Ta and H attached to a C in a Schrock carbene.[74]

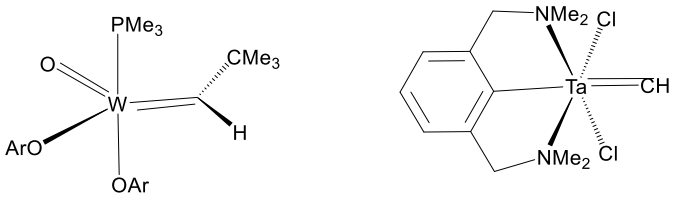

Figure 19. Examples of complexes with electon counts below 18. Left (electron count is 14, W(IV) oxidation state), Right (electron count is 12, Ta(III) oxidation state). [72]

1.2.2 Fischer carbenes

Fischer carbenes are most clearly defined by their singlet state, though there are other distinctive features. Fischer synthesised the first carbene complex in 1964 by attack of lithium alkyl on a metal carbonyl complex, followed by methylation (Scheme 7).[64]

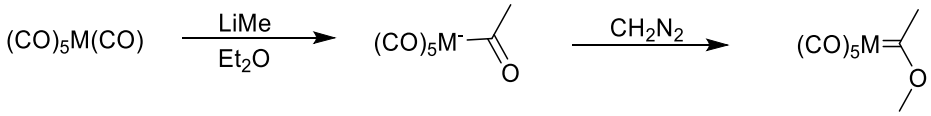

Scheme 7. Synthesis of the first Fischer carbene complex.[64]

There are some main factors that can indicate if a carbene ligand is a Fischer carbene, such as binding to a late transition metal with a low oxidation state, or π-acceptor and π-donor substituents attached to the carbene carbon. Fischer carbenes benefit from substituents that can donate electron density

into the empty π orbital on the carbon of the carbene, leading to an element of double bonding character between the carbon of the carbene and the substituent (which is usually a heteroatom such as oxygen or nitrogen). As a result, the carbene has a slight positive charge and behaves in an electrophilic manner (Figure 20).

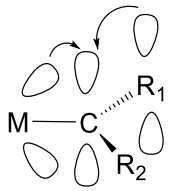

Figure 20. Diagram of orbitals involved in a M-Fischer carbene bond. R_1 is a substituent able to π donate into the empty carbon atom. In some cases, R_2 can also π donate but for clarity this has been omitted.

The donation of the electron pair from the heteroatom stabilised Fischer carbenes can lead to restricted rotation around the C-R_1 bond, indicative of double bond character. This is fluxional and can be seen from NMR studies (the presence of the two isomers can be seen in the ^{1}H NMR) where interconversion of methoxymethyl carbenes is rapid at room temperature but can be slowed sufficiently at -40^{o}C (as shown in Scheme 8).[2]

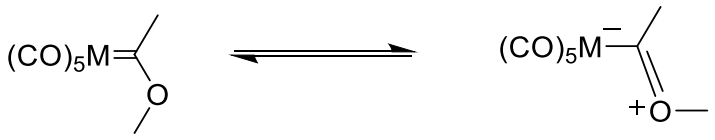

Scheme 8. Interconversion of Fischer carbene isomers that rapidly fluctuate at room temperature.[2]

1.2.2.1 N-Heterocyclic Carbenes

All Fischer carbenes mentioned prior to this point have been reactive and participate within reactions in which the M=C bond is broken. N-Heterocyclic carbenes (NHCs) like Fischer type carbenes (general structure shown in Figure 21) are in the singlet state because of the geometry of the five membered ring forces a sp^2 hybridisation on the system and the nitrogen heteroatoms can donate into the empty π orbital on the carbon (with their lone pair), whilst σ withdrawing effects (due to the larger electronegativity) lower the energy of the HOMO (Figure 22). These structures do not necessarily have to be in a five membered ring, there was an example of a four membered NHC developed in 2004, and there are also examples of rings of up to seven members.[75]

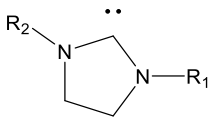

Figure 21. General structure of an N-heterocyclic carbene, where R_1 an R_2 can be a wide range of alkyl and aryl substituents and do not necessarily have to be the same, although they commonly are.

NHCs are stable and can act as spectator ligands, with tuneable electronic and steric properties. This has led to NHCs being regarded as phosphine analogues, but there are key differences. Thermodynamically NHC complexes are still less stable than their phosphine counterparts. This is due to bond length similarity between M-NHC and M-alkyl bonds, meaning they are prone to the same instabilities, resulting in a species that is at risk of reductive elimination, among other side reactions.[76,77]

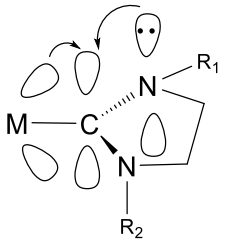

Figure 22. Diagram of nitrogen lone pair donating into the empty orbital of the carbon on the carbene (the orbital overlap and subsequent stabilisation from the other equivalent nitrogen atom have been omitted for clarity).

One of the most problematic side reactions is the tendency NHCs have to dimerise.[78] The first stable NHC was isolated in 1991 by Arduengo and co-workers (shown in Figure 23) and was stable due to both steric and electronic considerations. [79] The use of such a bulky ligand allows for kinetic stability previously unseen. Theoretically, the presence of the two nitrogen heteroatoms within the cyclic structure gives the structure the most stability against dimerisation when compared with phosphorous, oxygen or sulfur alternatives. This model however lacks more sophisticated consideration of the steric influences and effects on the overall system. Sterically bulky and demanding substituents at R_1 and R_2 (they do not necessarily have to be the same) can lead to further stabilisation to prevent dimerisation. The N-C-N bond angle in the five membered ring means that these substituents are "pulled apart" resulting in this being less impactful on the steric bulk at the central carbon centre than expected.[67]

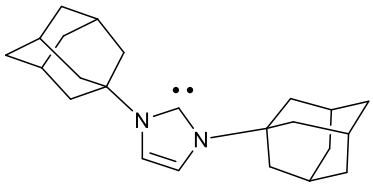

Figure 23. The first isolated stable N-heterocyclic carbene.

The mechanism of dimerisation is unlikely to proceed via a head on approach, which is suggested and supported by various research groups as early as from 1970.[80] There are two main suggestions of mechanisms which are consistent with kinetic and experimental data, which is an acid catalysed process in Scheme 9.[81]

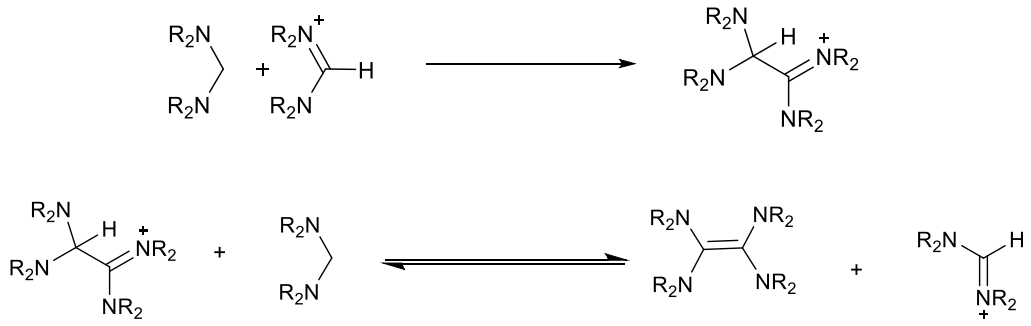

Scheme 9. Potential mechanism for proton catalysed dimerization of NHCs. R_1 and R_2 can be alkyl or aryl substituents.

The steric properties of NHCs can be categorised in a similar way to that of phosphines, using a method devised by Nolan, Cavallo and co-workers called the "buried volume" parameter.[82] Prior to this Nolan had attempted to develop a method similar to the Tolman steric parameter[83] for NHCs, which was based on crystallographic data. The method was checked for validity by examining the steric *versus* enthalpic relationship and was found to show a

"fair" correlation.[12] This model has highlighted the need for an improved method to calculate the steric parameter, leading to the creation of the "buried volume" parameter, which is defined as the percentage of a sphere occupied by the ligand on co-ordination to a metal (the sphere has a defined radius and the metal centre occupies the centre). The steric bulk of NHCs is "fan-like" with substituents attached to the heteroatoms within the ring close to the metal forming the percent buried volume parameter. It is worth noting that the buried volume parameter is calculated with the use of crystallographic data and therefore cannot be taken to be anything other than reflective of the solid state complex.[84] This "fan-like" arrangement of the substituents on the tertiary amines leads to an intrinsic anisotropy within NHCs. The components do not have consistent behaviour in each dimension/direction and as such restrictions must be placed on the NHC if any complex it is in, is being used for asymmetric catalysis.[67]

The electronic properties of NHCs can be categorised by the Tolman Electronic Parameter (TEP)[12], which works by measuring the infra-red stretching frequency of carbonyl ligands in an appropriate metal carbonyl (and ligand of interest) complex.[83,85] The TEP gives an overview of the donor and acceptor properties of a ligand. As the electron donating ability of the ligand increases, the electron density on the metal centre also increases, leading to an increase in π back-bonding to the carbonyl ligands resulting in a weaker CO bond and a decreased stretching frequency. NHCs are typically more electron donating

than their phosphine counterparts and therefore have stronger bonds to metal centres.

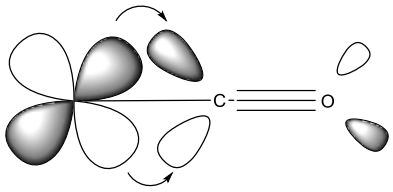

Figure 24. Diagram of π backbonding between a metal $d_{zx/y}$ with the CO π orbital.*

These properties of NHCs makes them particularly interesting to pursue as spectator ligands in catalysts or to try and isolate unique metal species. They have been explored in a variety of processes (such as Heck and Suzuki cross-coupling, olefin metathesis, hydrosilation, hydrogenation and hydroformylation.)[86–90]

1.2.2.2 Cyclic Alkyl Amino Carbenes (CAACs)

First discovered in 2005 cyclic alkyl amino carbenes (CAACs) were developed by Bertrand and co-workers.[91] Similar in structure to NHCs, but with a quaternary carbon centre in place of one the nitrogen centres, CAACs have very different electronic properties (Figure 25).

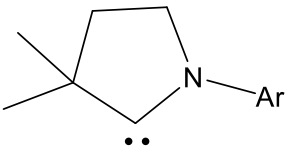

Figure 25. The basic structure of a CAAC, with a quaternary carbon and N present within the ring as the key features. The ligand is highly variable with substitution of different groups available around the molecule.

Computational studies have indicated that the HOMO- LUMO separation for CAACs (45 kcal mol^{-1}) is smaller than the HOMO-LUMO separation observed for NHCS (68 kcal mol^{-1})[92]. This is due to the substitution of one of the nitrogen atoms (an electronegative substituent, and π donor) with a quaternary carbon (which provides only σ donation). The electronic properties can be experimentally determined with the TEP method (previously mentioned in regards to NHCs) in combination with another technique (involving either the formation of a P or Se CAAC adduct and measuring the change in shift in the corresponding ^{31}P NMR spectra or ^{77}Se NMR spectra. This allows for an estimation of the π accepting or donating ability of the parent CAAC) taking into consideration the π accepting properties of the ligand, to give a value that allows for an estimation of the σ donating properties of a ligand (Figure 26).[93] Numerous reviews indicate that CAACs have the one of the largest π accepting abilities of any ligands, making them suitable for stabilisation of many low oxidation state metals.[92,94]

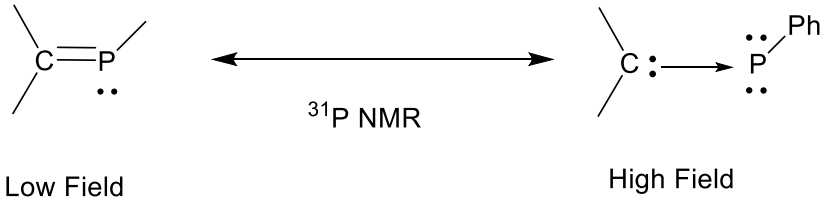

Figure 26. Diagram illustrating how the shift of how the phosphorous adduct reflects the electronic behaviour of the carbene. Low field shift indicates that the carbene has a strong π accepting ability and the bond is like a double bond, whereas a high shift indicates a weak π accepting ability.[93]

Transition metal complexes featuring CAAC ligands are nowhere near as heavily investigated as their NHC counterparts, and those that have been investigated are usually within catalysis (There are also a few cases where CAACs have been used for stabilising low co-ordinate metal centres).[95–98]

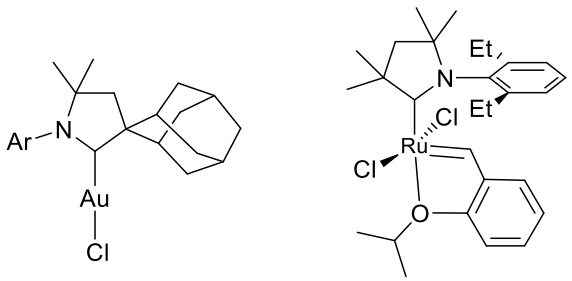

(3) **(4)**

Figure 27. Two examples of complexes containing CAACs capable of catalytic reactions.[99–101]

In 2007 **(4,** in Figure 27) was synthesised by Bertrand and co-workers, and was shown to be stereoselective for the formation of *Z*-olefins in cross metathesis reactions (with substrates *Z*-1,4-diacetoxy-2-butene and allyl benzene, in

relation to commercially available catalysts) and had the highest turnover number (TON) that had been reported at the time.[99,100] Complex **(3)** has been reported to be one of only a few complexes able to catalyse the intermolecular addition of dialkylamines to internal alkynes.[101]

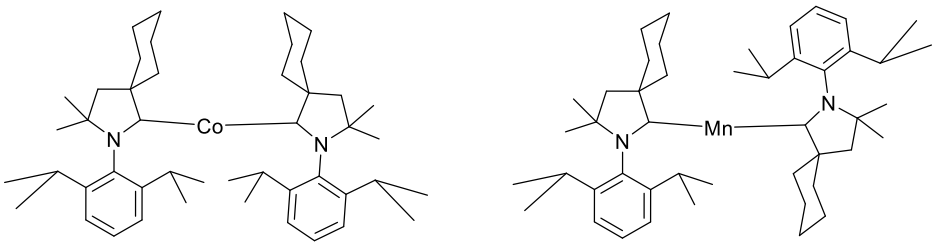

Figure 28. Examples of low co-ordinate species achieved with the aid of a CAAC ligand.[102]

Due to the low-lying LUMO of CAAC ligands (caused by the quaternary carbon centre only providing σ donation), back donation of the metal centre into carbon atom of the carbene is more favourable and can lead to stabilisation of low oxidation states (for example the Co and Mn complexes shown in Figure 28).[102]

1.3 Nitrogen/Pyridines as ligands

The use of nitrogen based monodentate ligands to stabilise low co-ordinate transition metal centres is vastly underexplored in the literature. There is an example of a four co-ordinate palladium complex containing two pyridine ligands that has been studied with the aid of DFT, with the aim of understanding the effect of labile monodentate ligands on mechanism of direct dioxygen coupled Pd oxidation catalysis.[103] There is a significantly greater number of examples for bidentate, amido and other chelating type pyridine-based ligands and specifically imino pyridine type ligands (Figure 29).[104]

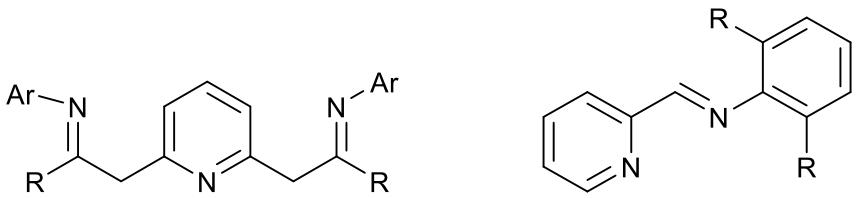

Figure 29. Two examples of imino pyridine ligands. The nitrogens within the structure than can co-ordinate to the metal centre. The example on left is tridentate and the example on the right is bidentate. R can be any alkyl group and Ar can be any aryl group. [104,105]

Monodentate pyridine ligands remain relatively unexplored in low co-ordinate chemistry. A recent paper by Power and co-workers discussed binding energies of a range of molecules usually associated more with solvation than co-ordination and comments specifically of the lack of reported iron pyridine three co-ordinate species. In addition the binding energy of pyridine is larger than previously thought.[106] Pyridine ligands may be lesser used as ligands within low co-ordinate chemistry, as the ligands usually need to be bulky and bond tightly to the metal. As pyridine ligands are usually considered weakly binding (though

recent works suggests the bonding is not as weak as first indicated) due to their σ donating and π accepting properties, they are less investigated compared to ligands like phosphines or previously mentioned NHCs within low co-ordinate transition metal complexes.[107]

1.4 Aims and objectives

The overall aim of this project was to increase the number low-coordinate open-shell complexes, in order to expand the library of complexes for investigation in structural chemistry, small molecule activation/catalysis and in magnetism. The use of low-coordinate complexes in these areas highlights the potential for the exploitation of their low-coordination and high reactivity. The development of new ligands in order to manipulate the properties of low co-ordinate complexes and reactivity is also of significant importance. The overall aims of the project were to be met by achieving the following objectives:

1) The use of the *m*-terphenyl ligand 2,6-$Mes_2C_6H_3^-$ to synthesise a variety of metal halides (of Mn, Fe, Co and Zn) to be used as precursors for the formation of substituted heteroleptic species.

2) The synthesis of a new small cyclic alkyl amino carbene and its potential co-ordination to create low co-ordinate heteroleptic complexes. Many homoleptic carbene complexes have been explored, while the heteroleptic complexes are far less so.

3) Synthesis of a selection of novel mixed *m*-terphenyl/pyridine heteroleptic complexes, since low co-ordinate complexes containing

neutral monodentate nitrogen donor ligands are an underexplored within the literature.

2. Results and Discussion:

2.1 m-terphenyl ligand synthesis

The ligand precursor [2,6-$Mes_2C_6H_3Li]_2$ was prepared according to the synthesis developed in 1996 by Saednya and Hart.[49] 2,6-$Mes_2C_6H_3I$ **(7)** was prepared from 1-bromo-2,4,6-trimethylbenzene that had been heated to reflux in a suspension of magnesium in THF to create the corresponding Grignard reagent, orange/brown solution **(5)** was used without further purification.

^{n}BuLi (2.5M in hexane) was added dropwise to a solution of 2,6-dichlorobenzene in THF at –78°C and stirred for a further 2 hours to allow for full deprotonation. MesMgBr **(5)** was added dropwise to the solution, where it was heated to reflux at 80°C for 16 hours. The solution was cooled to 0°C and iodine was added to quench the reaction to give 2,6-$Mes_2C_6H_3I$ **(7)** after work up and recrystallisation. Lithium halogen exchange using ^{n}BuLi afforded [2,6-$Mes_2C_6H_3Li]_2$ in 27% yield.

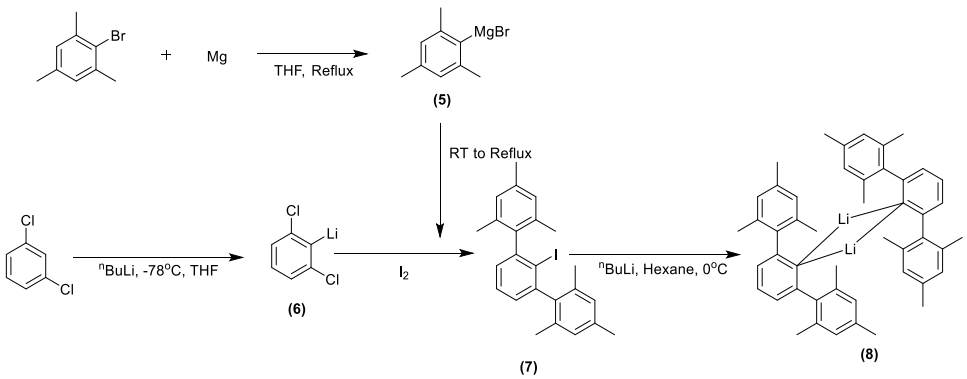

Scheme 10. Overall synthesis of m-terphenyl precursor complex [2,6-$Mes_2C_6H_3Li]_2$.[49]

2.2 CAAC Ligand synthesis

The attempted CAAC synthesis was based on a method developed by Guy Bertrand in 2007.[108] The four step procedure is shown below. LDA is usually used in the second step as well as for the deprotonation in the final step to create the carbene. The second step however requires the use of ^{n}BuLi with Me_2NH for the reaction to successfully proceed.

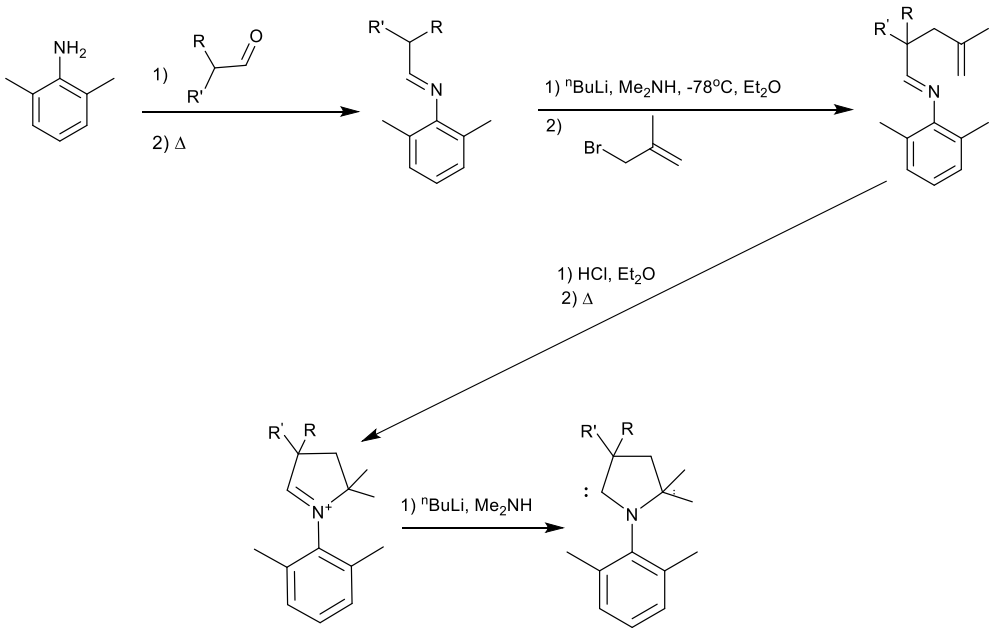

Scheme 11. CAAC synthesis adapted from ref [108]

The initial synthesis of the imine was attempted by a variety of methods, all of which were treated in the presence of air and gave poor yielding and impure solutions. This was confirmed by comparisons of ^{1}H NMR data, with the addition of a mesitylene internal standard to determine the exact yields obtained in solution. The common impurities appeared to be a result of

incomplete conversion of the starting materials to the desired imine (isobutylaldehyde/isovaleraldehyde, and 2,4,6-trimethyl aniline/2,6-dimethyl aniline). Purification by distillation was limited due to the similar boiling points of the desired product and the aldehyde. Purification *via* column chromatography was also attempted. Despite the number of eluents trialled, the column chromatographyon acidic silica and basic alumina only provided limited success, the products obtained was still too impure. The use of Dean-Stark apparatus for the condensation reaction between the amine and aldehyde was also attempted using a catalytic amount of tosic acid, which showed limited conversion of starting materials to the desired product (as seen in Scheme 12). A procedure involving Na_2SO_4 and *N,N*-dimethylbenzylamine as a catalyst with 2,6-dimethylaniline and isovaleraldehyde reacting at 0°C was then attempted (see Scheme 14). This process proved inefficient giving a yield of 14% and the product was of low purity, and contained the aldehyde starting material as an impurity, as determined by NMR spectroscopy.

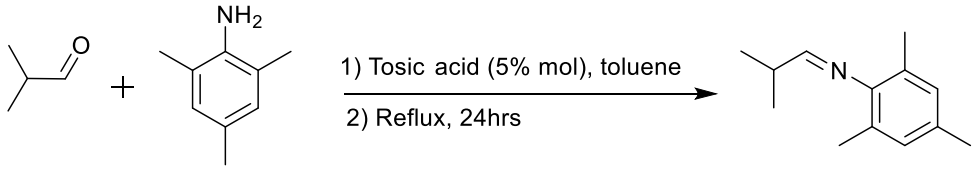

Scheme 12. First attempted synthesis of linear imine.

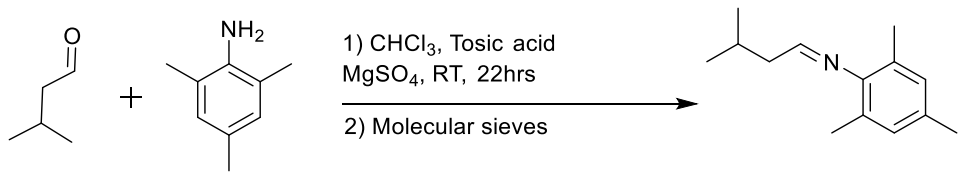

Scheme 13. Second attempted synthesis of the linear imine.

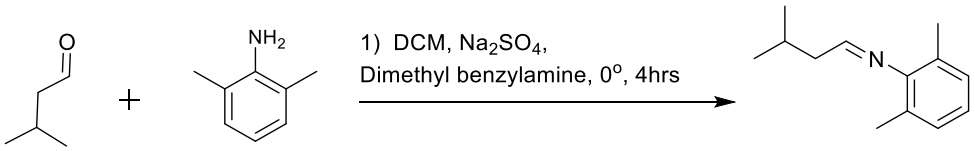

Scheme 14. Third attempted synthesis of linear imine.

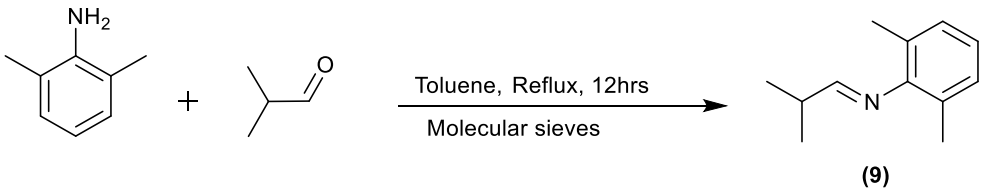

Scheme 15. Successful synthesis of linear imine

The synthetic route that was successful and produced a pure product is detailed below. Isobutylaldehyde was added dropwise to a solution of 2,6-dimethyl aniline in toluene containing 4 Å molecular sieves. The solution was then heated to reflux at 110°C for 12 h and allowed to cool before filtration to give a colourless, clear solution. The molecular sieves were washed with hexane to extract as much imine as possible and combined with the filtrate. The product **(9)** was purified by removal of solvent *in vacuo* and then trap to trap distillation under vacuum. The product was characterised using ^{1}H NMR

spectroscopy which showed six peaks corresponding to the different environments in the product.

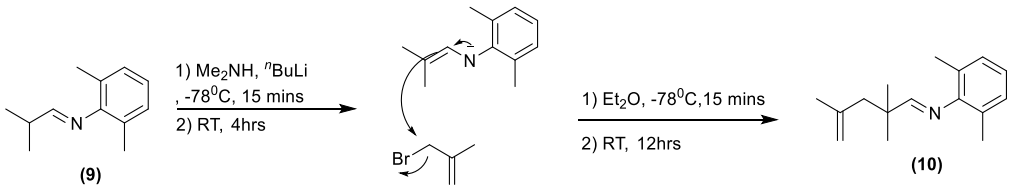

Scheme 16. Alkylation of the imine prior to cyclisation.

The imine **(9)** used was deprotonated with a solution of Me_2NLi in Et_2O at –78°C added dropwise (Scheme 16). This solution was held at low temperature for 15 mins, then stirred at room temperature for a further 4 h. Solvent and volatiles were removed *in vacuo*, and the cream solid residue was solvated in Et_2O to give a clear yellow solution and cooled to –78°C. 3-Bromo-2-methylpropene was added dropwise and the resultant pale-yellow suspension was stirred at low temperature for a further 15 mins. The solution was allowed to warm to room temperature and stirred for 12 h. Volatiles were removed *in vacuo* to give a cream precipitate.

The product **(10)** was extracted from hexane to give an orange/brown oil as the product. The product was characterised with comparative ^{1}H NMR and ^{13}C NMR spectra of the starting materials and the product. The product has 9 peaks ^{1}H NMR in the spectrum, with a distinctive shift in imine proton from 7.76 to 7.61ppm, whilst the introduction of peaks at 4.90 and 4.76ppm belong to the protons at the carbon double bond (HSQC spectra of the proton and carbon

also supports this, showing both protons coupling to the same carbon). Small amounts of starting materials were also present (≈20%).

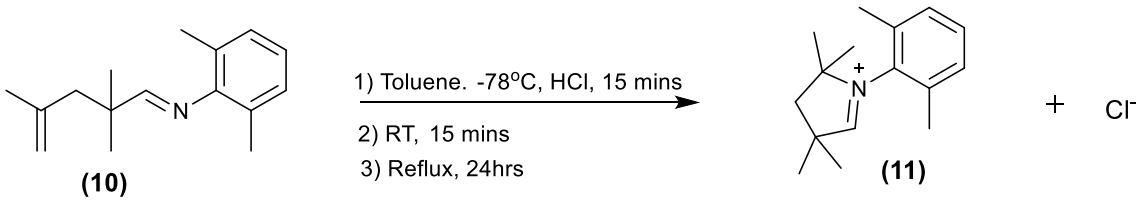

Scheme 17. Cyclisation of imine.

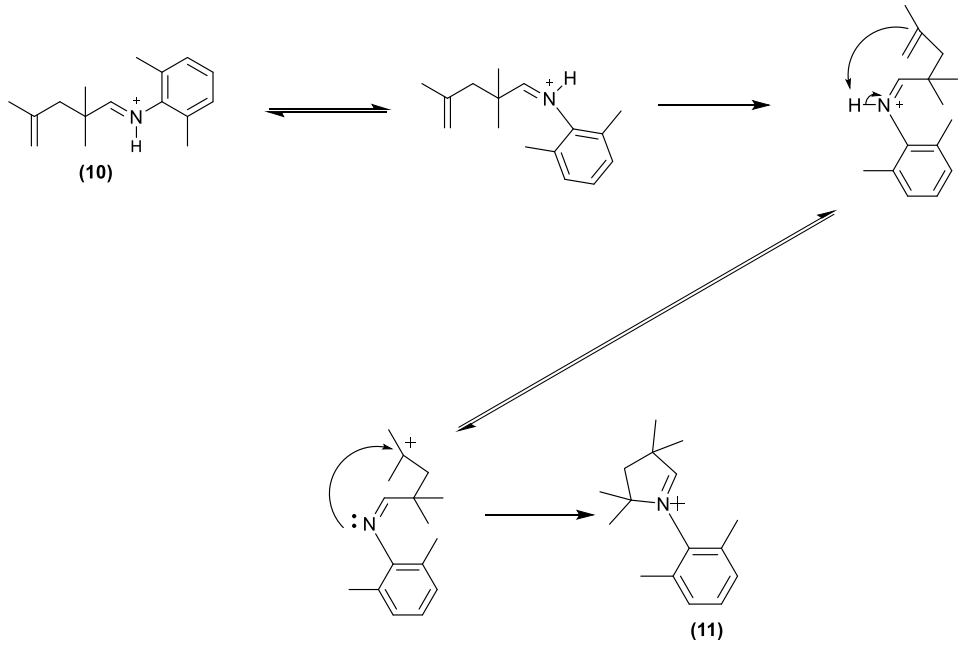

Scheme 18. Potential mechanism of cyclisation of imine.[109,110]

A solution of HCl in Et_2O (2.5 M, 2 ml) was added dropwise to a solution of pre-cyclised imine **(10)** in toluene (*circa* 10 ml) at –78˚C and stirred for 15 mins (Scheme 17). Precipitation of a cream white solid was observed as the solution was allowed to warm and stir at room temperature for 15 mins. The solution was then heated to reflux at 110˚C for 24 h to give an orange solid and clear orange solution. Volatiles were removed *in vacuo* to give an orange/brown oily

solid which was purified to a brown oily solid by distillation. The product was characterised by ^{1}H NMR showing a distinctive shift in the proton peak for the imine (from 7.61 to 10.56ppm). Other key features include the loss of the peaks at 4.90 and 4.76ppm (which indicates successful cyclisation as the double bond system is no longer present.) The product appeared pure with no other major peaks that those expected in the proton spectra. This information indicates that there are few protic impurities within the sample but other impurities could be present.

The acid (HCl) H^{+} protonates the imine nitrogen, leading to the formation of a cation (Scheme 18). This positively charged N then can isomerise the imine which can then rearrange to form a carbocation, which is most stable at the tertiary carbon centre. This carbocation is then attacked by the N lone pair leading to ring closure and the formation of the five membered ring.[109,110]

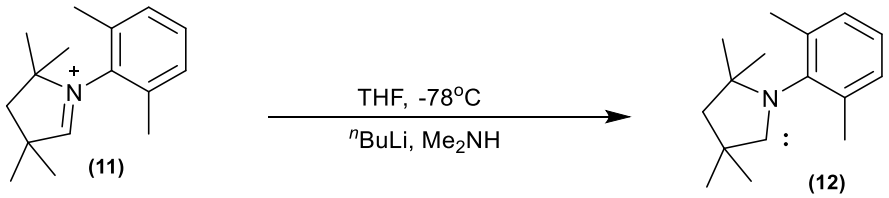

Scheme 19. Deprotonation of cyclic imine to produce a CAAC

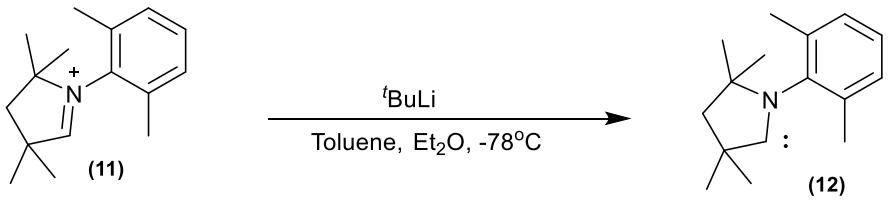

Scheme 20. Deprotonation of cyclic imine to produce a CAAC with $^{t}BuLi$

Deprotonation of the cyclic imine **(11)** was attempted with Me_2NLi at –78°C, this initial attempt was unsuccessful and showed no indication of the intended carbene product (Scheme 19) by ^{1}H and ^{13}C NMR spectroscopies. Instead of removal of the proton on the carbene, this proton showed a shifted upfield due to nucleophilic attack. The reason for this appears to be due to the ability of Me_2NLi to act as a base *versus* a nucleophile due to its lack of steric bulk. A base less prone to nucleophilic attack was also attempted because of this finding, $^{t}BuLi$, but this again met with no success (Scheme 20). The ^{1}H NMR in this case again indicated that nucleophilic attack was occurring, though the presence of other proton peaks in the particularly in the alkyl region, could mean multiple reactions were likely occurring alongside this. CAAC molecules with larger groups on the *ortho*-position of the flanking aryl group (a selection of which can be seen in Figure 30) have been synthesised and have been used to create homoleptic species. The small CAAC attempted here may be too sterically unhindered, leaving the carbon open to nucleophilic attack by all bases regardless of their own steric bulk.

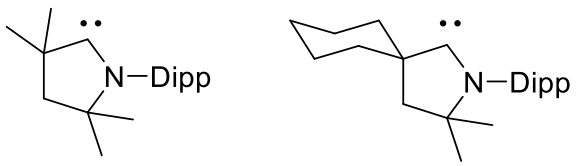

Figure 30. Examples of stable CAACs synthesised.[94]

2.3 Metal-halogen bridged dimer synthesis

The synthesis of the transition metal halide-bridged species closely followed the synthesis developed by Power and co-workers in 2007.[35] Although this was used as a precursor for the synthesis of metal- metal multiply bonded species, such species can be broken apart by the addition of a suitable ligand to lead to the creation of a low co-ordinate species. The reaction is a salt metathesis reaction and leads to the formation of a lithium halide as a by-product and provides a driving force for the reaction to proceed.

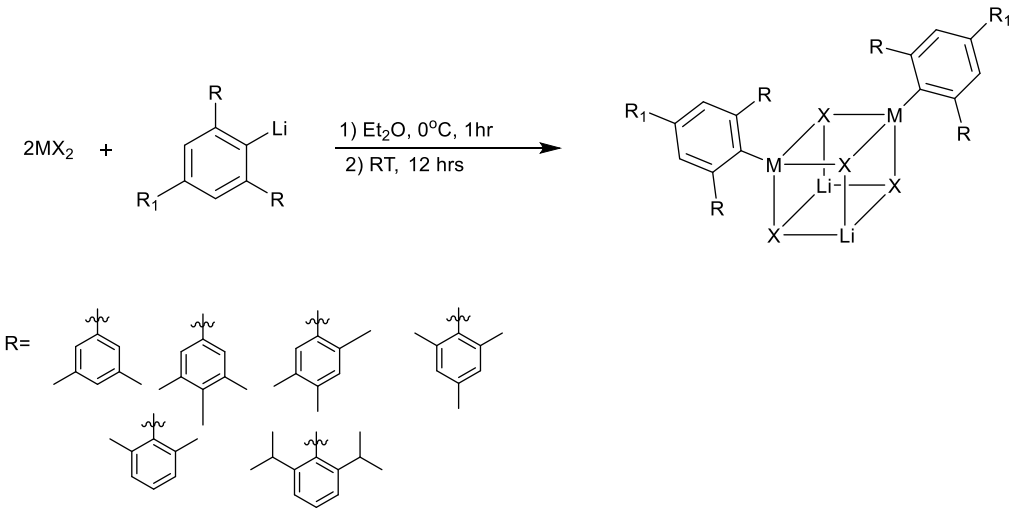

Scheme 21. General scheme for the synthesis of metal halogen bridged dimer species synthesised as precursors for further co-ordination. Alteration of R affects the steric properties, shown above are a selection of possible R groups though others are also possible but only 2,4,6-Mes was used within this project (they are presented as known examples of substituents). R_1 can be varied to include most substituents that can affect both steric and electronic properties.

$[2,6\text{-}MesC_6H_3Li]_2$ was dissolved in diethyl ether to create a clear yellow solution, which was added dropwise to a stirring solution of either $ZnCl_2$, $MnBr_2$,

$FeBr_2$ or $CoBr_2$ in diethyl ether at 0°C. The solution was kept at low temperature for 1 h and then allowed to warm to room temperature to stir for a further 16 h. Volatiles were removed *in vacuo* to give a cream solid (in the case of zinc and manganese, cobalt and iron were green/blue and brown/yellow respectively). The product was extracted into cyclohexane to remove the lithium halide and left to crystallise at 0°C. The compounds that did not yield crystalline material after this time, were dried *in vacuo* to form powdery solids and NMR spectroscopy was used to monitor the success of the reaction, and all were used without further purification. The slow addition of lithiated ligand to the metal halide solution (in combination with the ratio of starting materials) limits the production of homoleptic two co-ordinate species and should lead to the formation of the cubane structure seen above.

$[Mes_2C_6H_3CoBr]_2.[LiBr(OEt_2)]_2$ **(13)**, $[Mes_2C_6H_3FeCl]_2.[LiCl(OEt_2)]_2$ **(14),** $[Mes_2C_6H_3MnBr]_2.[LiBr(OEt_2)]_2$ **(15)**, $[Mes_2C_6H_3ZnCl]_2.[LiCl(OEt_2)]_2$ **(16)** precursors were synthesised, with one crystal structures obtained displaying the general "cubane" structure **(13)** seen in (Scheme 21). The remaining complexes **14-16** do not have crystallographic data and only have ^1H NMR spectra, which does not give structural information. The assignment of the structures of the complexes **14-16** therefore is tentative and based on the crystallographic data present for **13** and similar complexes in the literature.

Zinc compound **(16)** is the only complex of the four that is diamagnetic and so its formation can be followed by NMR spectroscopy in a quantitative manner. Complex **(16)** was less pure than desired, due to the low solubility of **(16)** in hydrocarbon solvents which are typically used to separate them from the lithium salt by-product.[111] Due to the lack of crystalline material for X-ray analysis it is hard to know if the exact structure is a cubane for all of the reactions (particularly the zinc precursor **(16)**), it is possible in some cases for the product to be a halide bridged dimer instead. **(13-15)** are paramagnetic samples which exhibit ^{1}H NMR spectra with resonances that range from (100 to -100 ppm).

Crystals were obtained for the cobalt bromide-bridged dimer **(13),** as clear green/ blue needles (structure shown in Figure 31).

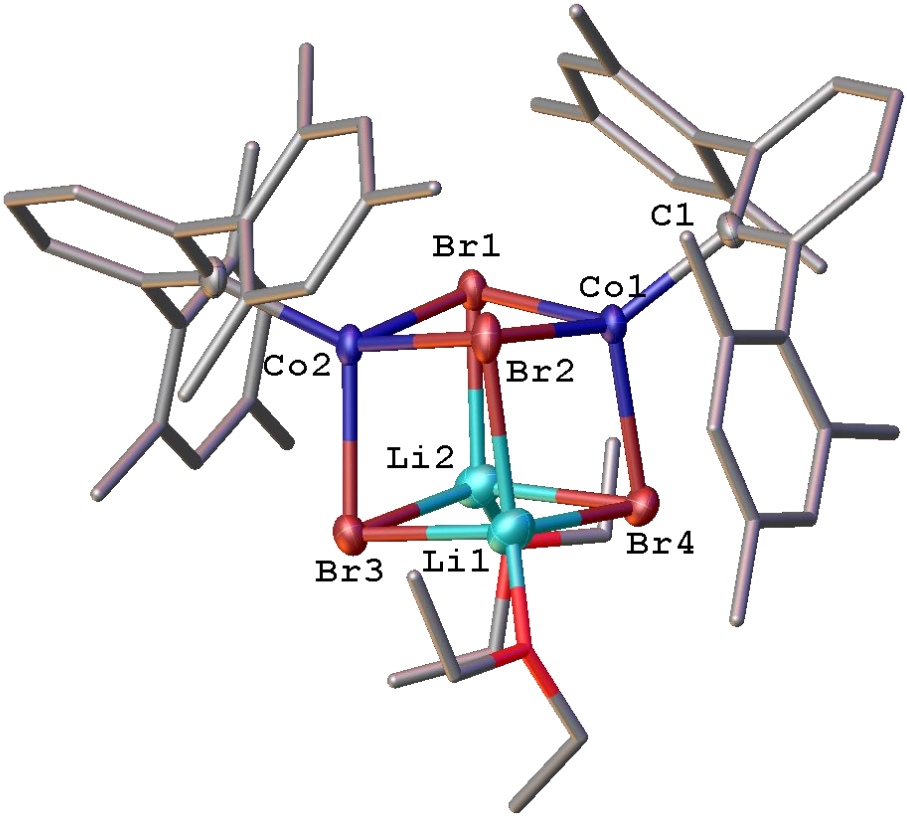

*Figure 31. Structure of the Co bromide bridged dimer species **(13)**. The species takes a cubane structure that is distorted with half of the above molecule existing in the asymmetric unit. Co is four co-ordinate, bonded to three bromides and one terphenyl ligand (Co(1) and Co(2) are equivalent). Hydrogen atoms have been omitted for clarity. The displacement ellipsoids are set to a 50% probability level (Only on the main cube of the structure for clarity).*

Similar structures have been observed in the literature[112,35] with the distinctive cubane structure first seen in 2007 (of the form $[Li(OEt_2)\{C_6H_3\text{-}2,6\text{-}(C_6H_3\text{-}2,6\text{-}{}^{i}Pr_2)_2\}MI_2]$ where M= Mn, Fe or Co), but dimeric examples have been seen before.[51] Complex **(13)** is consistent with the data obtained from these complexes, crystallising in the same space group, and with a similar motif (the only differences arise from the halide within the cube, solvent or each substituent on the *m*-terphenyl).

The difference in angles and bond lengths between the components of the cube (Co^{2+}, Br^{-} and Li^{+}) lead to a distortion in the regular shape. This distortion is a consequence of the difference of sizes between Br^{-} (1.96 Å), Co^{2+} (0.70 Å) and Li^{+} (0.76 Å) ions,[113] as well as the presence of the terphenyl ligand bound to the cobalt (these ionic radii are for a co-ordination number of 6). The cobalt is in a four-co-ordinate distorted tetrahedral arrangement and in the (II) oxidation state. The C(1)-Co(1)-Br(2) angle is 120.63(11)° and is significantly wider than the usual 109.5° for a regular tetrahedron, due to the steric bulk and hindrance placed on the cobalt centre by the nearby terphenyl which forces the angle to be larger to accommodate this large ligand. The species is dimeric, with two metal centres connected by the bridging halide.

The τ_4 value can be used to assess the geometry of a resulting complex as tetrahedral or square planar, given by the equation shown below.

$$\tau_4 = \frac{360 - (\alpha + \beta)}{360 - 2\theta} \approx -0.00709\alpha - 0.00709\beta + 2.55$$

$$\alpha, \beta = largest\ angles\ in\ structure, \qquad \theta = 109.5°$$

For the structure above (Figure 31) the cobalt atoms are in a configuration that gives a value of 1, confirming the distorted tetrahedral geometry. Another similar equation for the value τ'_4 takes into consideration different values of α

and β to give a value that is better at discriminating between structures that could potentially give the same τ_4 value.

$$\tau'_4 = \frac{\beta - \alpha}{360 - \theta} + \frac{180 - \beta}{180 - \theta} \approx -0.00399\alpha - 0.01019\beta + 2.55$$

$$\beta > \alpha = Largest\ angles\ in\ structure, \qquad \theta = 109.5°$$

The τ'_4 value calculated is 0.94, which as a value close to 1 and the value of τ_4 previously obtained which indicates there are no other interactions in the co-ordination sphere.

No solvent is incorporated into the crystal structure aside from the diethyl ether co-ordinated to the lithium ions. The Co(1)-Co(2) centres are separated by a distance of 3.4438(8) Å and are only joined by the bridging bromide atoms, whilst being shielded by the terphenyl ligand to limit the co-ordination number. In the literature it has been shown that in similar complexes, the two metal centres are not completely independent of each other and can couple to each other. Coupling can result in a ferromagnetic or antiferromagnetic behaviour, where the overall μ_{eff} value of the complex can be increased or decreased respectively.[114]

Atoms	Bond Length Å	Bond Angle °
Br(1)-Co(1)-Br(3)	-	92.0(2)
Br(2)-Co(1)-Br(3)	-	96.19(3)
Br(2)-Li(1)-Br(4)	-	96.3(3)
Co(1)-Br(3)-Co(2)	-	86.57(3)
C(1)-Co(1)-Br(2)	-	120.63(11)
Co(1)-Br(1)	2.5198(9)	-
Co(1)-Br(2)	2.4750(9)	-
Co(1)-C(1)	1.994(4)	-
Br(1)-Li(1)	2.575(8)	-
Co(1)-Co(2)	3.4438(8)	-

*Table 2. Bond length and angles for the Co-Br bridged dimer species **(13)**.*

2.4 Synthesis of Donor-stabilised Complexes

The metal halogen bridged dimers synthesised previously, were used as precursors for the creation of heteroleptic complexes stabilised with donor molecules. The ligand of choice was added in a 2:1 ratio to the precursor to give a selection of three to four co-ordinate species (Scheme 22).

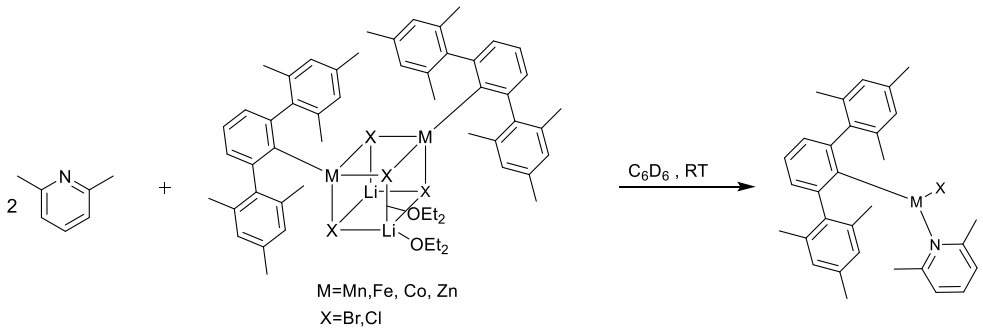

Scheme 22. General reaction for the synthesis of heteroleptic complexes

NMR scale reactions were used predominantly as larger scale synthesis methods attempted were met with limited success, showing mainly the

presence of starting materials. Reactions involving the iron (II) halide-bridged dimer and 2,6-lutidine have not yet produced crystals, and due to the paramagnetic nature of the samples, structures can only be inferred based on those previously obtained. The structures appear to take one of two forms, a four co-ordinate dimeric structure where the halogen bridge is maintained and a monomeric three co-ordinate structure (Figure 32).

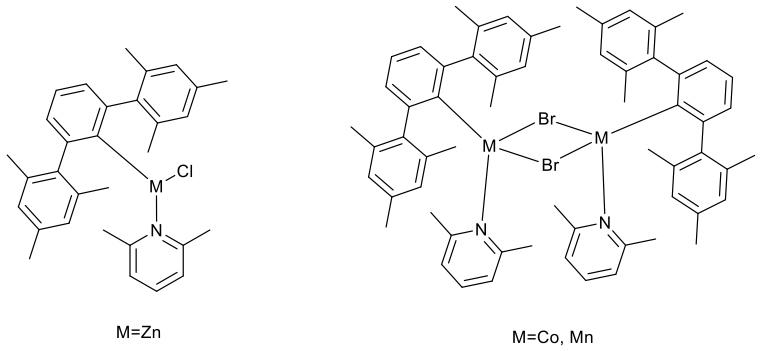

Figure 32. General diagrams of the solid state structure of the products obtained confirmed with the use of X-ray crystallography.

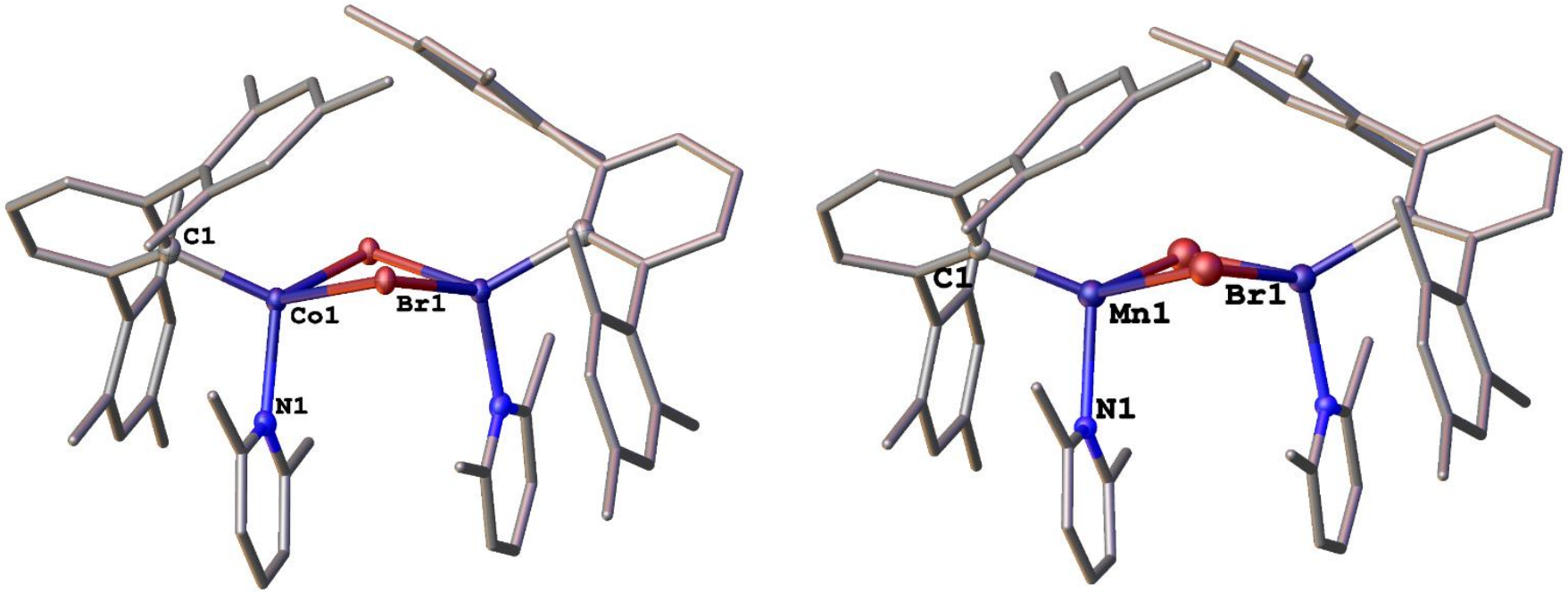

Figure 33. Crystal structures from left to right, cobalt 2,6-lutidine dimer species $[Co_2Br_2(Me_2C_5H_3N)_2(2,6\text{-}Mes_2C_6H_3)_2]$ ***(17)****, Manganese 2,6-lutidine structure* $[Mn_2Br_2(Me_2C_5H_3N)_2(2,6\text{-}Mes_2C_6H_3)_2]$ ***(18).*** *Crystals* ***(17)*** *and* ***(18)*** *display the cis conformation. Crystals* ***(17)*** *and* ***(18)*** *co-crystallised with pentane which (like the hydrogens on all structures) has been omitted for clarity. The displacement ellipsoids are set to a 50% probability level.*

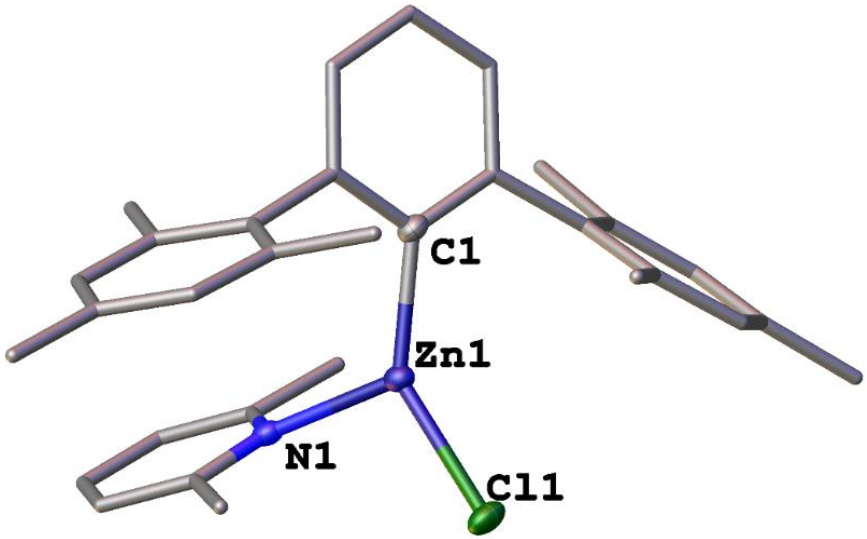

Figure 34. Zinc complex 2,6-lutidine [ZnCl($Me_2C_5H_3N$)(2,6-$Mes_2C_6H_3$)] ***(19).*** *No solvent co-crystallised with* ***(19)****, and all hydrogens have been omitted for clarity. The displacement ellipsoids are set to a 50% probability level.*

Atoms	Bond Length (Å)	Bond Angle (°)
Br(1)-Co(1)-Br(2)	-	87.201(14)
Co(1)-Br(1)-Co(2)	-	88.082(14)
C(1)-Co(1)-N(1)	-	109.31(5)
N(1)-Co(1)-Br(1)	-	114.98(4)
Co(1)-Br(1)	2.4934(5)	-
Co(1)-N(1)	2.1226(12)	-
Co(1)-C(1)	2.0302(14)	-
Co(1)-Co(2)	2.4902(5)	-

*Table 3. Bond lengths in Å and angles in ° for structure **(17)***

Atoms	Bond Length (Å)	Bond Angle (°)
Br(1)-Mn(1)-Br(2)	-	88.26(12)
Mn(1)-Br(1)-Mn(2)	-	88.76(12)
C(1)-Mn(1)-N(1)	-	108.0(7)
N(1)-Mn(1)-Br(1)	-	112.7(4)
Mn(1)-Br(1)	2.635(4)	-
Mn(1)-N(1)	2.320(16)	-
Mn(1)-C(1)	2.09(2)	-
Mn(1)-Mn(2)	2.634(4)	-

*Table 4. Bond lengths (in Å) and angles (in °) for structure **(18)**.*

Atoms	Bond Length (Å)	Bond Angle (°)
Cl(1)-Zn(1)-N(1)	-	103.49(14)
N(1)-Zn(1)-C(1)	-	116.9(2)
C(1)-Zn(1)-Cl(1)	-	139.51(17)
Cl(1)-Zn(1)	2.1998(17)	-
N(1)-Zn(1)	2.083(5)	-
C(1)-Zn(1)	1.978(6)	-

*Table 5. Bond lengths (in Å) and angles (in °) for structure **(19)***

Atoms	Bond Length (Å)	Bond Angle (°)
Br(1)-Co(1)-Br(2)	-	89.92(6)
Co(1)-Br(1)-Co(2)	-	90.08(6)
C(1)-Co(1)-O(1)	-	109.2(3)
O(1)-Co(1)-Br(1)	-	101.5(2)
Co(1)-Br(1)	2.481(2)	-
Co(1)-O(1)	2.021(7)	-
Co(1)-C(1)	2.053(8)	-
Co(1)-Co(2)	2.481(2)	-

*Table 6. Bond lengths (in Å) and angles (in °) for the reported structure labelled **(20)**. See Figure 35.* [51]

Despite the additional co-ordination within the cobalt and manganese precursors **(17)** and **(18),** the halide bridge is retained, in addition to the *cis* conformation adopted by the 2,6-lutidine molecules. In the literature a similar structure **(20)** (with THF rather than 2,6-lutidine) was synthesised in 1996[51] and adopts the *trans* conformation (Figure 35). The structures are similar enough, with the maintained presence of the halogen bridge, that they can be compared. As 2,6-lutidine is more sterically demanding than THF, it may be expected that the halide bridge would be broken and a three co-ordinate species (with regards to the metal centre) could be synthesised, similar to that seen for the zinc containing structure **(19)**. THF however is not aromatic or planar, and hence is bulkier than 2,6-lutidine as a ligand, which could be part of the reason for the *trans* conformation adopted.

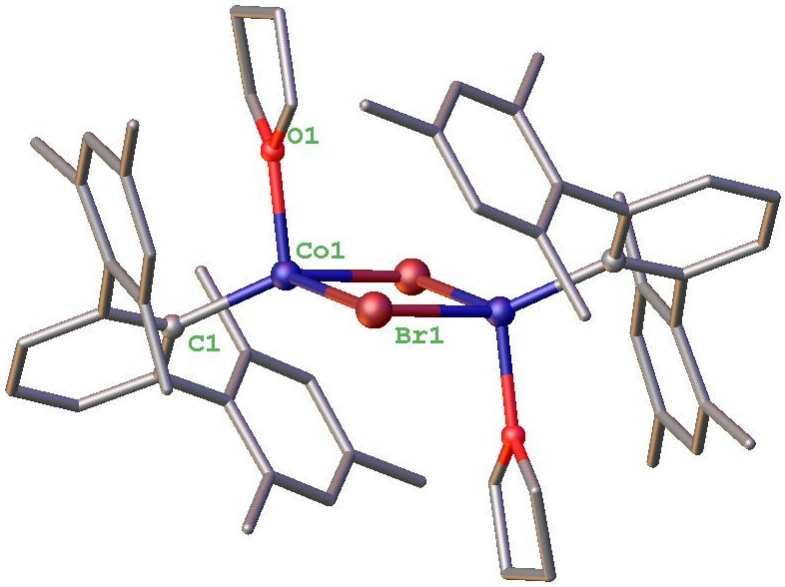

*Figure 35. Similar structure to **(17)** and **(18)** containing THF rather than 2,6-Lutidine, where the halogen bridge is maintained but the conformation is trans rather than cis.*[51]

In addition to sterics, the *cis* conformation seen may also be due to the presence of CH-π interactions which cause a stacking effect between the methyl group on the 2,6-lutidine with a face of the Mes flanking group on the terphenyl. For **(17)** the distance between a H from the Me substituents (on the 2,6-lutidine) and the plane (the Mes group) is 2.54 Å, while for **(18)** the distance is 2.60 Å, both of which are in the accepted range of 2.5-2.7 Å for a CH-π bonding interaction.[115,116] This effect is also displayed between units, with the methyl substituents on the terphenyl ligand able to a stack with one of the faces of the Mes groups.

Structure	τ_4	τ'_4
17	0.96	0.94
18	0.99	0.97
19	-	-
20	1	1

*Table 7. Table containing the T_4 and T'_4 values for complexes **17-20**.*

All τ_4 and τ'_4 values are close to 1 and consistent indicating there are no other bonding interactions within the co-ordination sphere (Table 7).

The M-N average bond length across the period decreases as follows, Mn (2.32 Å) > Co (2.12 Å) > Zn (2.08 Å) and are all within known range of bond lengths.[117,118] Comparison of these bond lengths to those in the literature, is difficult due to the low co-ordination number of the complex. Regardless the three co-ordinate species $[M\{N(SiMe_3)_2\}_2(NC_5H_5)]$ containing pyridine

synthesised in 2017, show smaller bond lengths than is seen here.[106] However the complexes **(17)** and **(18)** are in a four co-ordinate geometry, and generally an increase in co-ordination is accompanied by an increase in bond length.[118] The M-C bond lengths across the period also decrease with Mn (2.09 Å)> Co (2.03 Å) > Zn (1.98 Å) and are consistent with previously reported similar structures (values for these bond lengths range from 2.095(3)-2.108(2) for Mn, 2.001(3)-2.014(2) for Co). [40,51,52]

Structure **(19)** is a monomer whereas structures **(17)** and **(18)** are dimeric. It would be reasonable to think that as size generally decreases across a period, this trend would be reflected in the ionic radius (ionic radii of Zn(II) =0.74 Å; for Mn(II) and Co(II)=0.70 Å).[113] The halogen has changed from Cl^- (1.84 Å) to Br^- (1.96 Å), so this will also contribute to whether a monomer or dimer is observed in the solid state (All ionic radii given are for a co-ordination number of 6).[113] All of the precursors with the exception of **(16)** contain a bridging halide, whilst due to the small size of the Cl^- ion is a monomer (no halide-bridge), which may contribute to formation the monomeric three co-ordinate product **(19)**. If the same reaction had been repeated with the I^- or even Br^- halide-dimer precursor, the product may also be a dimer. The sterics of each component may contribute to the co-ordination of the complex, but electronics may also have an effect.

The magnetic moments for both **(17)** and **(18)** were determined using Evans method**,** giving values for μ_{eff} of 1.26 μ_B and 1.20 μ_B respectively.[119] These values are lower than would be expected as **(18)** would have to be a low spin monomer in solution to fit this value (this is highly unlikely given that manganese low spin complexes are rare and the splitting energy Δ_{tet} is smaller than Δ_{oct}. Most octahedral manganese complexes are high spin, so it is improbable that the pairing energy of the electrons would be smaller than this value.)[120] The value for **(17)** is also low. As a technique, Evans is highly dependent on many factors, including concentration and temperature.[121] Due to issues with weighing in a glove-box, and the purity of the complex being undetermined, these values are tentative. The measurements also lacked the necessary repeats, to make them reliable values, before taking into consideration that temperature is also a necessary factor to consider for truly accurate values to be obtained.

2.5 Di-*tert*-butyl pyridine complexes

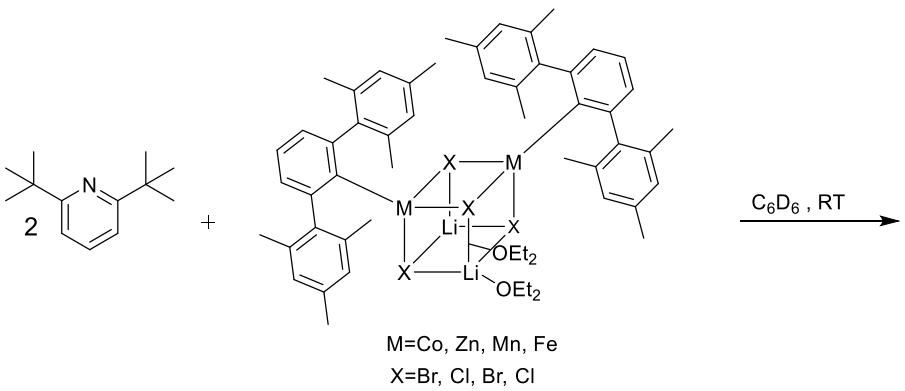

Scheme 23. Small scale synthesis of di-tert-butyl pyridine complexes.

Given the dimeric formulations observed for **(17)** and **(18)**, the steric demands of the pyridine ligand was increased, and 2,6-di-*tert*-butylpyridine was utilised for this (Scheme 23). Unfortunately, no 2,6-di-*tert*-butylpyridine complexes were successfully crystallised. Synthesis of these complexes was carried out on a small scale as larger scale reactions attempted were met with extremely limited success (the majority component of final reaction mixture was starting material). The NMR data indicates a reaction had occurred and from the crystallographic data previously obtained with the corresponding 2,6-lutidine structures, it is possible to infer a structure. Due to the increased steric bulk of the di-*tert*-butyl pyridine ligand, it may be expected are monomeric and of a three co-ordinate nature. The increased bulk on the di-*tert*-butylpyridine means that the metal centre will be more hindered and possible reduction of the metal centre with a suitable agent (KC_8, etc) could lead to isolation of a two co-ordinate species.

3. Conclusions

This thesis reports two distinct research projects; (i) the attempted synthesis of a new CAAC ligand, and (ii) the synthesis of new heteroleptic, first row transition metal complexes.

The synthesis of new CAACs presents the opportunity to expand the repertoire of this family of ligands, increasing the steric and electronic properties available when using these ligands. The development and attempted synthesis of a small and novel CAAC, was successful up until the final deprotonation step. This final step was investigated and deprotonation was attempted with a variety of different agents [Me_2NLi, ^tBuLi, $KC(N(SiMe_3)_2)$] to consistently indicate nucleophilic attack was the dominant reaction. Although this synthesis has, as yet, met without success, has provided valuable information for the synthesis of new ligands from this family.

The synthesis of four metal halogen precursors (Co with the crystallographic data so takes the form stated, whilst Mn, Fe and Zn are inferred from this structure and similar literature) $[Li(OEt_2)ArMX_2]_2$ (where M = Mn, Co, Fe and Zn; Ar = 2,6-$Mes_2C_6H_3$; X = Cl, Br) from the metathesis reactions of MX_2 with [2,6-$Mes_2C_6H_3Li]_2$ has been reported. These complexes were then reacted with two equivalents of 2,6-lutidine or 2,6-di-*tert*-butyl pyridine to give a variety of novel three and four co-ordinate heteroleptic complexes. Three of these complexes produced crystals with sufficient quality to allow the structure to be determined *via* X-ray diffraction measurements. The bromide-containing structures **(17)** and **(18)** retained the halogen bridging structure from the

precursor complex, and the co-ordinated 2,6-lutidine ligands are in a *cis* configuration. This is likely a consequence of the CH- π bonding interactions in the solid state. **(19)** differs from **(17)** and **(18)** as it is three co-ordinate in the solid state. The remaining complex structures have been inferred from analogy with the structures which have already been obtained and NMR spectroscopic data.

4. Future work

Further synthesis of the complexes is necessary, and, this project should be extended, to include cyclic voltammetry (which could be used to determine if the complex could be reduced to lower co-ordination numbers and what potentials would be required, as well as the degree of interaction between centres) EPR, IR, UV/Vis and Evans/SQUID measurements. Once the already synthesised species have been fully characterised, this study should be extended to other pyridyl ligands such as those featuring flanking aryl ligands in the 2- and 6-positions to imbue more steric protection around the low-coordinate metal centre. Although there has not been any success with the synthesis of the new CAAC in this Thesis, further carbene ligands such as those shown in Figure 36 could be utilised. These CAACs are more sterically encumbering and have been successfully synthesised and not explored outside of homoleptic complexes.

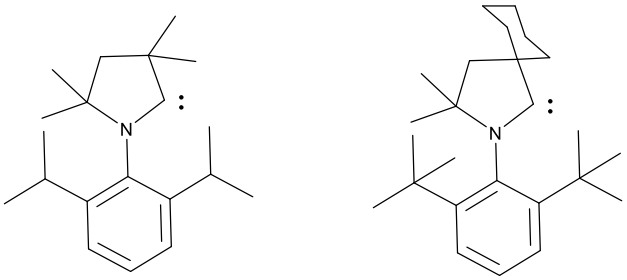

Figure 36. Two CAAC structures seen within the literature. The CAAC on the left is commercially available.

$ZnBr_2$ or ZnI_2 could be used to synthesise a zinc halide-bridged dimer precursor that could then be reacted with 2,6-lutidine and 2,6-di-*tert*-butylpyridine. In the case of any zinc bromide precursor this could give a direct comparison to the manganese and cobalt complexes and their resultant structures. This would determine whether the monomer three co-ordinate species seen for the zinc chloride complex is indeed due to size effects across a period, or a combination of size effect across a period and halogen size.

Further investigations into expanding the known CAAC ligands should be undertaken. The synthesis of a more sterically encumbered CAAC and subsequent attempted co-ordination to transition metal complexes is sure to generate precursors for M(I) species, with successful reactions that produce heteroleptic complexes being reduced as shown in Scheme 24 (*e.g.* using KC_8 or Na depending on the measured reduction potential to attempt to reach even lower co-ordination numbers).

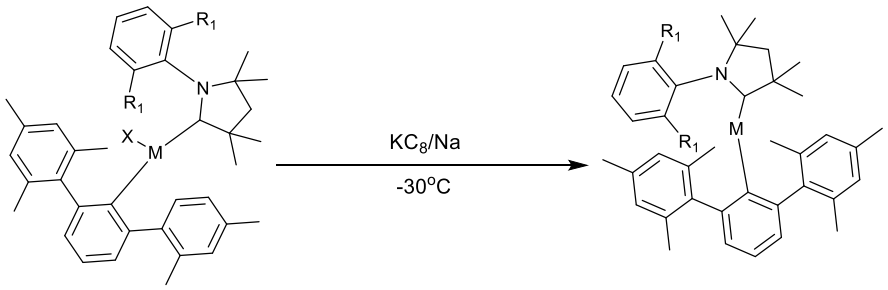

Scheme 24. Reaction scheme for reduction of a heteroleptic two co-ordinate species.

5. Experimental:

5.1 General Procedure

All experimental procedures were carried out in strict anaerobic and anhydrous conditions due to the air and moisture sensitive nature of the compounds involved. All manipulations were carried out using standard Schlenk and Glovebox techniques under argon or nitrogen.

Solvents were dried by refluxing for three days over molten potassium (toluene), sodium/benzophenone (THF) or Na/K alloy (diethyl ether). *n*-Pentane and *iso*-hexane were dried by passing the solvent through a drying column containing activated 4 Å molecular sieves. The solvents were stored in ampoules over a potassium mirror (toluene, diethyl ether, *n*-pentane, *iso*-hexane) with the exception of THF which was stored over activated 4 Å molecular sieves. Solvents were degassed *in vacuo* before use. Benzene-d_6 was heated to reflux over potassium for three days, vacuum transferred to another ampule and then degassed with three freeze-pump-thaw cycles before use. $CDCl_3$ was dried by heating to 85 °C over calcium hydride for three days, before being transferred to an ampule under vacuum where it was degassed with three freeze-pump-thaw cycles before use. 2,6-Lutidine was stored in an ampule over activated 4 Å molecular sieves and degassed before use. 2,6-Di-*tert*-butylpyridine was used as received.

5.1.1. NMR spectroscopy

Samples of air- and moisture-sensitive compounds were prepared either using glove

box techniques and contained in Young's tap modified borosilicate glass NMR tubes. All NMR data was collected on Bruker AV400 or AV(III)400 spectrometers. Chemical shifts are quoted in ppm relative to TMS (^{1}H, $^{13}C\{^{1}H\}$).

5.1.2 Mass Spectrometry

Air-sensitive samples for mass spectrometry were prepared under a N_2 atmosphere in the glovebox by placing the sample inside glass capillaries. These were then sent to the EPSRC National Mass Spectrometry Facility in Swansea. The LTQ Orbitrap XL was used to collect the mass spectrometry data, using Electrospray Ionisation (ESI) and Atmospheric Solids Analysis Probe (ASAP) techniques on either positive or negative ionisation mode. For ESI, samples were injected into or infused into a stream of methanol (50µL/min). Nebulisation is assisted by a flow of nitrogen through a sheath around the capillary. For ASAP, the sample is loaded inside in a glass capillary as a solid or solution, which is then heated from ambient temperature (40° C) until the sample vaporises (Corona discharge current is at 4 µA).

5.1.3 X-Ray Crystallography

Under a flow of N_2, crystals suitable for X-ray diffration were quickly removed from the Schlenk and covered with Fomblin (YR-1800 perfluoropolyether oil).

A suitable crystal was then mounted on a polymer-tipped MicroMount™ and cooled rapidly to 120K in a stream of cold N_2 using an Oxford Cryosystems open-flow cryostat.[122] Single crystal X-ray diffraction data were collected either using an Agilent SuperNova diffractometer, Atlas CCD area detector (mirror-monochromated Cu-Kα radiation source; λ = 1.54184 Å; ω scans), an Agilent SuperNovaII diffractometer, Atlas S2 CCD area detector, or an Agilent SuperNovaII diffractometer Titan S2 CCD area detector (mirror monochromated Cu-Kα radiation source; λ = 1.54184 Å; ω scans). Absorption corrections were applied using an analytical numerical method (CrysAlis Pro). All non-H atoms were located using direct methods and difference Fourier syntheses. Hydrogen atoms were placed and refined using a geometric riding model. All fully occupied non-H atoms were refined with anisotropic displacement parameters, unless otherwise specified. Crystal structures were solved and refined using the OLEX2[123] software packaging and SHELXL[124] and CIF-checked in conjunction with Prof. Alexander Blake, Dr William Lewis, Gareth Ashworth, Roberto Nolla Saltiel.

5.2 *m*-Terphenyl ligand synthesis

2,4,6-$Me_3C_6H_2MgBr$ (5)

Magnesium turnings (3.31 g, 0.163 mol) were activated by stirring for 30 mins in acetone (*circa* 50 ml) to which iodine (50 mg, 0.197mmol) was added. The solid was collected and washed with acetone (*circa* 3 x 50 ml) and dried in the

oven for a further 30 mins before being ground overnight *in vacuo*. THF (*circa* 150 ml) was added to the magnesium turnings and a solution of bromomesitylene (19.23 ml, 0.163 mol) in THF (*circa* 150 ml) and added dropwise. The resultant solution was heated to reflux for 4 h and then left to cool/settle overnight. The mixture was filtered to give a clear orange liquid (27.9 g, 0.125 mol, 76 %) as the product, which was used directly in the next stage of synthesis.

2,6-$Mes_2C_6H_3I$ (7)

1,3-Dichlorobenzene (5.54 ml, 0.0485 mol) was diluted with THF (*circa* 300 ml) and cooled to –78 °C. ^{n}BuLi (2.5 M in hexanes) (21.4 ml, 0.0535 mol) was added dropwise to this solution and stirred at –78°C for a further 2 h, followed by slow dropwise addition of a solution of **(5)** (27.9 g, 0.125 mol) in THF (*circa* 300 ml). The resulting solution was left to warm to room temperature and then heated to reflux overnight at 80 °C for 16 h. The solution was then left to cool to room temperature and further cooled to 0 °C before iodine (20 g**,** 0.079 mol) was added in 3 portions over 30 mins to quench the reaction. The purple solution was diluted further with diethyl ether (*circa* 200 ml) and sodium sulfate was added (*circa* 200 ml) leading to the solution changing to a pale yellow colour. The solution was divided into two portions (due to the quantity of liquid) and deionised water is added (*circa* 100 ml) before extraction with diethyl ether (2x100 ml). The organic phase was then washed with deionised water (2x100 ml) and brine (100 ml). The organic phases were then combined and dried with

magnesium sulphate, filtered and had solvent removed *in vacuo* to give a pale-yellow solid (10.94 g, 27 %) as the product.

The ^{1}H NMR data is below and matches the reported spectra.[125]

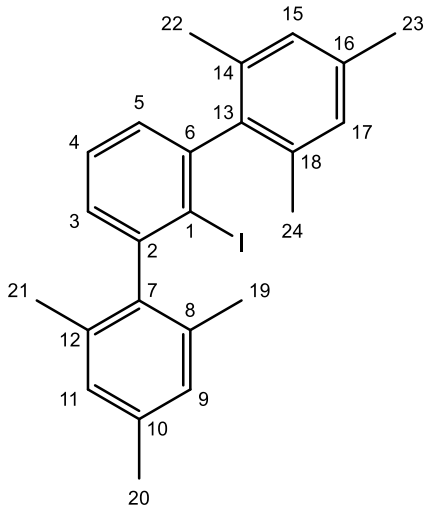

^{1}H NMR (400MHz, $CDCl_3$,298K): **δ**(ppm): 7.46 (t, 1 H, J= 7.56 Hz, **(4)**), 7.08 (d, 2 H, J=7.48 Hz, **(3, 5)**), 6.96 (s, 4 H, **(9, 11, 15, 17)**), 2.35 (s, 6 H, **(20, 23)**), 1.98 (s, 12 H, **(19, 21, 22, 24)**).

^{13}C NMR (400MHz, $CDCl_3$, 298K): **δ** (ppm): 147.3 **(1)**, 142.2 **(7,13)**, 137.4 **(10, 16)**, 135.5 **(2,6)**, 129 **(4)**, 128.2 **(9, 11, 15, 17)**, 127.9 **(3, 5)**, 107.7 **(8, 12, 14, 18)**, 21.4 **(20, 23)** , 20.4 (**19, 21, 22, 24)**

[2,6-$Mes_2C_6H_3Li]_2$ (8)

2,6-$Mes_2C_6H_3I$ (10.93 g, 0.01308 mol) was dried overnight and then solvated in hexane (*circa* 50 ml) and cooled to 0 °C. ^{n}BuLi (2.5 M in hexanes) (7.87 ml, 0.01962 mol) was added dropwise and left stirring at 0°C for 1 h. The solution

was allowed to warm to room temperature and left stirring overnight for 16 hrs. The product was filtered and dried to give a white/cream powder (5.44 g, 8.49 mmol, 64.9 %).

The ^{1}H NMR spectra is below and matched the literature.[49,125]

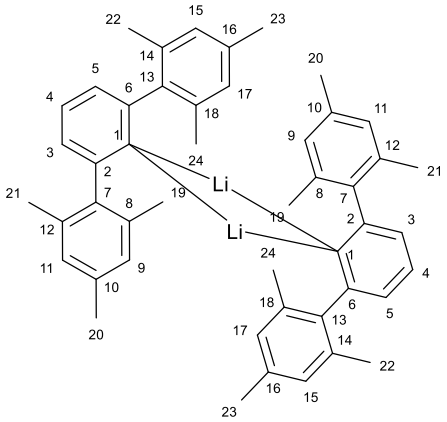

^{1}H NMR (400MHz, C_6D_6, 298K): **δ** (ppm): 7.24 (t, 1H, J=7.89Hz, **(4)**), 6.84 (s, 4H, **(9,11,15,17)**), 6.82 (d, 2H, J=7.95Hz, **(3,5)**), 2.17 (s, 6H, **(20,23)**), 1.83 (s, 12H, **(19,21,22,24)**)

^{13}C NMR (400MHz, C_6D_6, 298K): **δ** (ppm): 173.5 **(1)**, 151.81, 142.90, 136.05, 136.00, 129.37 **(9,11,15,17)**, 125.85 **(4)**, 123.50 **(3,5)**, 21.24 **(19,21,22,24)**, 20.82 **(20,23)**.

5.3 CAAC Synthesis

Imine synthesis **(9)**

Isobutylaldehyde (11 ml, 0.121 mol) was added dropwise to a solution of 2,6-methylaniline (15 ml, 0.121 mol) in toluene (*circa* 10 ml) and active 4 Å

molecular sieves (*circa* 10 g). The solution was set to reflux at 100°C for 12 hrs. The resultant slurry was filtered and washed with hexane (*circa* 20ml). Solvent was removed *in vacuo* and the product was distilled under vacuum at 100°C to obtain the product as a clear colourless solution (21 ml, 0.105 mol, 87 %)

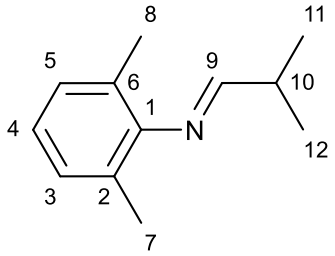

^{1}H NMR (400MHz, $CDCl_3$, 298K): **δ** (ppm): 7.76 (d, 1H, J= 4.6 Hz, **(9)**), 7.27 (d, 2H, J= 7.56 Hz, **(3,5)**), 7.15 (t, 1H, J=7.8 Hz, **(4)**), 2.94 (septet of doublets, 1H, J=6.88, 4.76 Hz, **(10)**), 2.36 (s, 6H, **(7,8)**), 1.51 (d, 6H, J= 6.88 Hz, **(11,12)**)

^{13}C NMR (400MHz, $CDCl_3$, 298K): **δ** (ppm): 172.00 **(9)**, 170.02, 150.88, 142.65, 128.05 **(3,5)**, 127.78, 126.48, 123.10 **(4)**, 121.26, 34.65 **(10)**, 18.84 **(11,12)**, 17.90 **(7,8)**.

Pre-cyclised Imine (10)

Me_2NLi (0.28 g, 5.45 mmol) in THF (*circa* 10 ml) was added dropwise to a solution of **9** (1 ml, 5.45 mmol) in Et_2O (*circa* 7 ml) at -78°C. The clear colourless solution was stirred at -78°C for a further 15 min and a clear yellow colour change was seen, followed by formation of a white precipitate. The solution

was allowed to warm to room temperature and stirred for four hrs, wherein the precipitate redissolved and the solution turned to clear yellow. The solvent is removed *in vacuo* to give a cream solid with an orange oil. This was dissolved in Et_2O (*circa* 15 ml) and the solution was cooled to -78°C to give a clear yellow colour. 3-Bromo-2-methylpropene (0.55 ml, 0.5.45 mmol) was added dropwise and formation of a precipitate was observed. The solution was stirred at -78°C for 15 min and then at room temperature for 12 h. Solvent was removed *in vacuo* to give a cream solid in a pale yellow solution. This mixture was washed with hexane and filtered to give a pale orange/ yellow solution. The volatiles were removed *in vacuo* to give a pale orange oil (0.85 g, 3.49 mmol, 68 %).

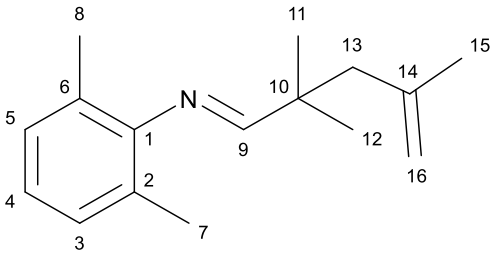

^{1}H NMR (400MHz, $CDCl_3$, 298K): δ (ppm): 7.61 (s, 1H**, (9)**), 7.03 (d, 2H, J= 7.33 Hz, **(3,5)**), 6.91 (t, 1H, J=7.59 Hz, **(4)**), 4.90 (s, 1H, **(16)**), 4.76 (s,1H, **(16)**), 2.32 (s, 2H, **(13)**), 2.10 (s, 6H, **(7,8)**), 1.82 (s, 3H, **(15)**), 1.28 (s, 6H, **(11,12)**)

^{13}C NMR (400MHz, $CDCl_3$, 298K): δ (ppm): 174.39 **(9)**, 151.72 **(1)**, 142.72 **(14)**, 128.09 **(3, 5)**, 126.83 **(2, 6)**, 123.37 **(4)**, 114.93 **(16)**, 48.16 **(13)**, 40.84 **(10)**, 25.25 **(11,12)**, 24.97 **(15)**, 18.34 **(7, 8)**

Cyclised Imine (11)

A solution of HCl in Et_2O (2.5 M, 1.86 ml, 3.71 mmol) was added dropwise to a solution of pre-cyclised imine (0.85 g, 3.71 mmol) in toluene (*circa* 10 ml) at -78°C. The solution showed formation of precipitate and was stirred at -78°C for a further 15 min. The solution was allowed to warm to room temperature for 15 min and then heated to reflux at 110°C for 24 h. Volatiles were removed *in vacuo* and a trap to trap distillation was used to remove some of the remaining impurities to give a brown solid (0.925 g, 3.48 mmol, 94 %).

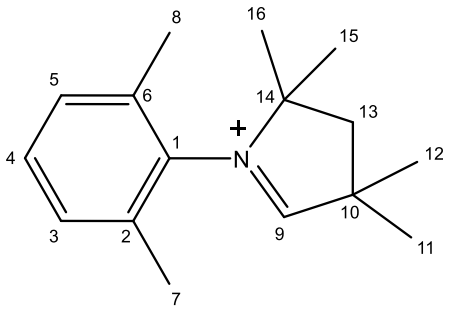

^{1}H NMR (400MHz, $CDCl_3$, 298K): δ (ppm): 10.56 (s, 1H, **(9)**), 7.35 (t, 1H, J= 7.28 Hz, **(4)**), 7.25 (d, 2H, J= 7.64 Hz, **(3,5)**), 2.37 (s, 8H, **(7,8) (13)**), 1.80 (s, 6H, **(15,16)**), 1.58 (s, 6H, **(11,12)**).

^{13}C NMR (400MHz, $CDCl_3$ 298K): δ (ppm): 193.80 **(9)**, 134.05 **(2,6)**, 132.88 **(1)**, 130.97 **(4)**, 130.25 **(3,5)**, 128.11, 123.50, 114.97, 83.77, 49.75 **(13??)**, 48.49 **()**, 48.18 **(10)**, 28.77 **(15,16)**, 27.46 **(11,12)**, 25.29, 20.00 **(7,8)**.

5.4 Cubanes:

$[Mes_2C_6H_3CoBr]_2.[LiBr(OEt_2)]_2$ (13)

$[2,6\text{-}Mes_2C_6H_3Li]_2$ (400 mg,0.56 mmol) was dissolved in Et_2O (*circa* 20 ml) and added dropwise to a solution of $CoBr_2$ (409 mg, 1.8 mmol) in Et_2O (*circa* 10 ml) at 0°C. The resultant solution was stirred at 0°C for 1 h and then left to warm to room temperature overnight. Solvent was removed in vacuo affording a green/brown solid. The product was extracted into cyclohexane (*circa* 10 ml) and recrystallised to give green crystals of pure product at –7°C (147 mg, 0.12 mmol, 21 %).

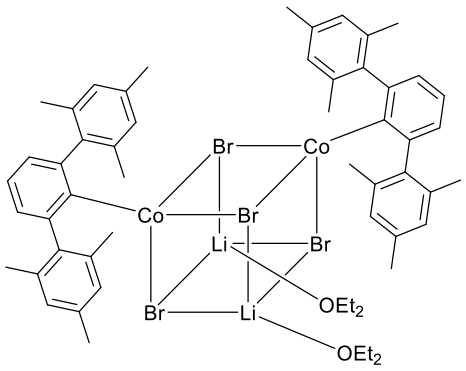

^{1}H NMR (400MHz, C_6D_6, 298K): δ (ppm) (all peaks appear as singlets): 22.57 (Δv=91 Hz), 7.27 (Δv=109 Hz), 6.89 (Δv= 110 Hz), 5.45 (Δv=120 Hz), 2.33 (Δv=64 Hz), 2.20 (Δv=52 Hz), 2.01 (Δv=76 Hz), 0.42 (Δv=62 Hz), -3.39 (Δv=67 Hz), -10.52 (Δv=76 Hz), -11.51 ((Δv=92 Hz).

Formula	$C_{56}H_{69}Br_4Co_2Li_2O_2$
Temperature (K)	120
M_w	1226.54
Crystal system	Monoclinc
Space Group	$P2_1/n$
a (Å)	11.6127(4)
b (Å)	26.0701(9)
c (Å)	18.6708(5)
α (°)	90
β *(°)*	91.470(3)
γ *(°)*	90
V *(Å^3)*	5650.6(3)
Z'	1
R_1 (%)	4.48
wR_2 (%)	11.65
Crystal dimensions (mm^3)	0.651 x 0.077 x 0.052
2θ range (°)	6.68 to 149.12
Measured reflections	24845
R_{int}	0.0448
Unique reflections	11242
Completeness of data (%)	99.96

*Table 2. Crystallographic data of the solid state structure of the Co bromide cubane structure **(13)**.*

$[Mes_2C_6H_3ZnCl]_2.[LiCl(OEt_2)]_2$ (16)

$[2,6\text{-}Mes_2C_6H_3Li]_2$ (400 mg,0.56 mmol) was dissolved in Et_2O (*circa* 20 ml) and added dropwise to a solution of $ZnCl_2$ (409 mg, 1.8 mmol) in Et_2O (*circa* 10 ml) at 0°C. The resultant solution was stirred at 0°C for 1 h and then left to warm to room temperature overnight. Solvent was removed *in vacuo* affording a white solid. Product was extracted into cyclohexane (*circa* 10 ml) and dried to give a white powder (0.365 mg,0.443 mmol, 80%).

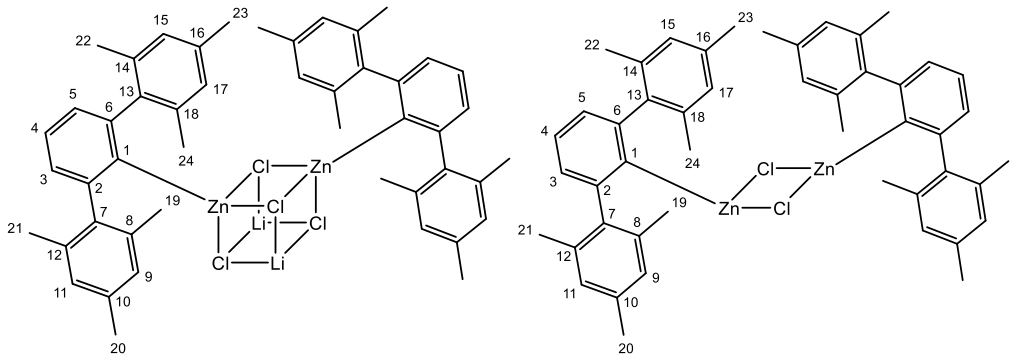

^{1}H NMR (400MHz, C_6D_6, 298K): δ (ppm): 7.25 (t, 2H, J = 7.56 Hz, (**4)**), 7.02 (d, 4H, J = 7.56 Hz, **3,5**), 6.87 (s, 8H, (**9,11,15, 17)**), 2.22 (s, 12H, **(20,23)**), 2.08 (s, 24H, **(19,21,2,24)**)

^{13}C NMR (400MHz, C_6D_6, 298K): δ (ppm): 141.62 **(2,6)**, 139.13 **(8,12,14,18)**, 136.09 **(10, 16)**, 135.43 **(7,13)**, 128.52 **(4)**, 128.16 **(9,11, 15, 17)**, 127.38 **(3,5)**, 20.77 **(20,23)**, 20.61 **(19,21, 22, 24)**

$[Mes_2C_6H_3MnBr]_2.[LiBr(OEt_2)]_2$ (15)

[2,6-$Mes_2C_6H_3Li]_2$ (400 mg,0.56 mmol) was dissolved in Et_2O (*circa* 20 ml) and added dropwise to a solution of $MnBr_2$ (236 mg, 1.8 mmol) in Et_2O (*circa* 10 ml) at 0°C. The resulting solution was stirred at 0°C for 1 h and then left to warm to room temperature overnight. Volatiles were removed *in vacuo* affording a cream solid. Product was extracted into cyclohexane (*circa* 10 ml) and dried to give a cream powder as the impure product (122 mg, 0.10 mmol, 18%).

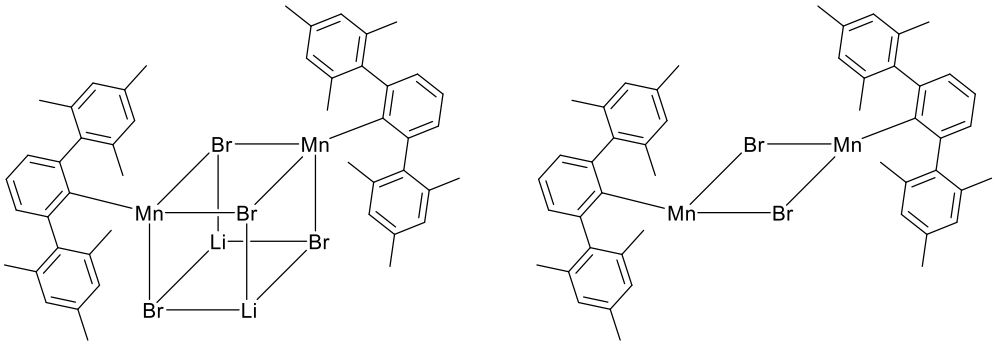

^{1}H NMR (400MHz, C_6D_6, 298K): δ (ppm) (All peaks are singlets): 7.01 (Δv=15 Hz), 6.88 (Δv=13 Hz), 6.77 (Δv=10 Hz), 3.25 (Δv=24 Hz), 2.21 (Δv=12 Hz), 2.08 (Δv=10 Hz), 1.40 (Δv=9 Hz), 1.12 (Δv=18 Hz), 0.30 (Δv=14 Hz).

$[Mes_2C_6H_3FeCl]_2.[LiCl(OEt_2)]_2$ (14)

$[2,6\text{-}Mes_2C_6H_3Li]_2$ (400 mg,0.56 mmol) was dissolved in Et_2O (*circa* 20 ml) and added dropwise to a solution of $FeCl_2$ (142 mg, 1.8 mmol) in Et_2O (*circa* 10 ml) at 0°C. The resultant solution was stirred at 0°C for 1 h and then left to warm to room temperature overnight. The solvent was removed *in vacuo,* affording a brown solid. This product was extracted into cyclohexane (*circa* 10 ml) and dried to give a green/brown powder (136 mg, 0.013 mmol, 7%).

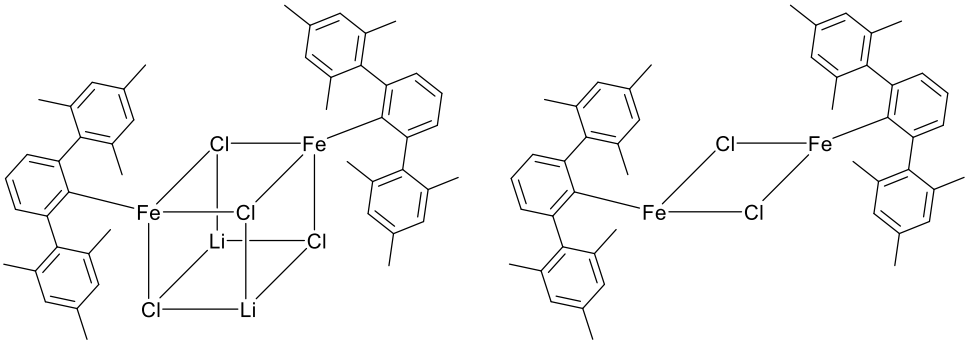

^{1}H NMR (400MHz, C_6D_6, 298K): δ (ppm) (all peaks appear as singlets) : 7.00 (Δv=18 Hz), 6.87 (Δv=16 Hz), 6.76 (Δv=12 Hz), 2.21 (Δv=12 Hz), 2.08 (Δv=12 Hz), 1.39 (Δv=11 Hz), 0.29 (Δv=13 Hz), -11.79 (Δv=46 Hz), -56.26 (Δv=158 Hz)

5.5 Synthesis of Pyridine Complexes:

$[Mes_2C_6H_3CoBr(2,6\text{-}MeC_5H_3N)]_2$ (17)

2,6-Lutidine (3.69 µl, 0.032 mmol) was added to a solution of $[Mes_2C_6H_3CoBr]_2.[LiBr(OEt_2)]_2$ (20 mg, 0.016 mmol) in C_6D_6 (0.6 ml). A colour change was observed from a deep green to a dark brown green. The product crystallised from a benzene/pentane diffusion experiment over one week at room temperature.

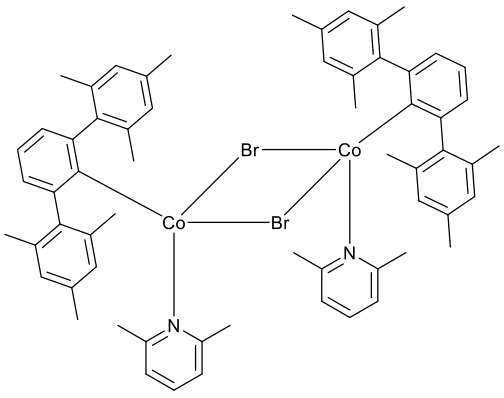

^{1}H NMR (400MHz, C_6D_6, 298K): δ (ppm) (all peaks are singlets): 24.90 (Δv=412 Hz), 7.28 (s), 7.00 (s), 6.94 (s), 6.73 (Δv=77 Hz), 3.44 (Δv=51 Hz), 2.61 (Δv=102 Hz), 2.33 (Δv=19 Hz), 2.21 (Δv=19 Hz), 1.51 (Δv=21 Hz), 1.26 (Δv=38 Hz), 0.40 (Δv=23 Hz)

μ_{eff}=1.257 μ_B

MS/ASAP *m/z*: $[M\text{-}2Br]^+$ calculated 958.4047, Found 955.5822.

[$Mes_2C_6H_3ZnCl(2,6\text{-}MeC_5H_3N)$] (19)

2,6-Lutidine (3.32 µl, 0.029 mmol) was added to a solution of $[Mes_2C_6H_3ZnCl]_2.[LiCl(OEt_2)]_2$ (15 mg, 0.014 mmol) in C_6D_6 (0.6 ml). No colour change was observed and white crystals were formed from benzene/pentane diffusion at room temperature in the glovebox over one week.

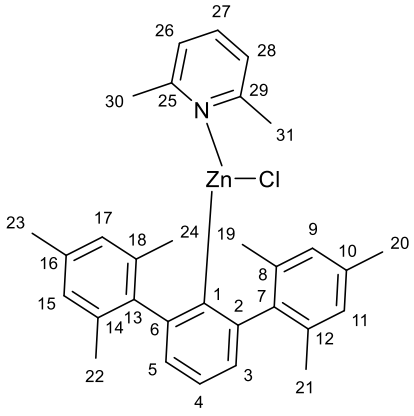

^{1}H NMR (400MHz, C_6D_6, 298K): δ (ppm): 7.34 (t, 1H, J = 7.52 Hz**, (4)**), 7.07 (d, 2H, J = 7.48Hz, **(3,5)**), 6.81 (s, 4H, J = 5.2 Hz, **(9,11,15,17)**), 6.29-6.06(br s, 2H,

ΔV=91 Hz, **(26,27,28)**), 2.22 (s, 12H, **(19,21,22,24)**), 2.18 (s, 6H, **(20,23)**), 2.06 (br s, 6H, ΔV=129.20 Hz, **(30,31)**).

^{13}C NMR (400MHz, C_6D_6, 298K): δ (ppm): 157.44, 154.13 **(4)**, 149.78 **(3,5)**, 147.63, 143.69, 142.22, 141.62, 139.16, 136.87, 136.26, 136.10, 135.72, 135.43, 135.03, 130.40, 128.75, 128.52, 126.43, 121.44, 65.91, 27.23, 24.00, 21.42, 21.16, 21.07 **(19,21,22,24)**, 20.80 **(20, 23)**, 20.15 **(30,31)**,

[$Mes_2C_6H_3MnBr(2,6\text{-}MesC_5H_3N)]_2$ (18)

2,6-Lutidine (3.69 µl, 0.032 mmol) was added to a solution of $[Mes_2C_6H_3MnBr]_2.[LiBr(OEt_2)]_2$ (20 mg, 0.016 mmol) in C_6D_6 (0.6 ml). No colour change was observed and small white crystals were obtained from benzene/pentane diffusion at room temperature in the glovebox over 2 weeks.

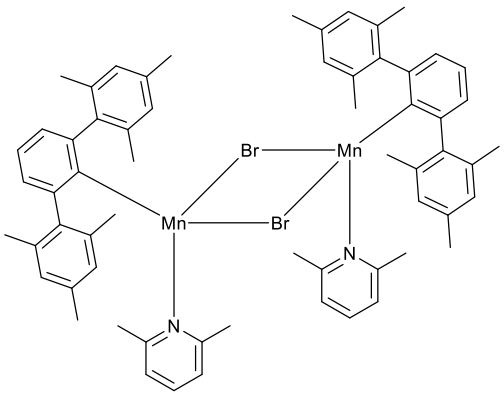

^{1}H NMR (400MHz, C_6D_6, 298K): δ (ppm) (all signals are singlets): 10.13 (Δv= 558 Hz), 7.28 (Δv=27 Hz), 7.13 (Δv=40 Hz), 6.99 (Δv=39 Hz), 6.90 (s), 3.39 (Δv=57

Hz), 2.33 (ΔV=44 Hz), 2.20 (Δv=35 Hz), 1.52 (Δv=19 Hz), 1.24 (Δv= 47 Hz), 0.41 (Δv=43 Hz).

μ_{eff}= 1.20 μ_B

Mass spec: Showed only the presence of protonated 2,6-$Mes_2C_6H_4$.

[$Mes_2C_6H_3FeCl(2,6\text{-}MeC_5H_3N)$] (21)

2,6-Lutidine (3.32 µl, 0.029 mmol) was added to a solution of $[Mes_2C_6H_3FeCl]_2.[LiBr(OEt_2)]_2$ (15 mg, 0.014 mmol) in C_6D_6 (0.6 ml). No obvious colour change was observed. Crystals are yet to be obtained.

^{1}H NMR (400MHz, C_6D_6, 298K): δ (ppm) (all peaks appear as singlets): 54.73 (Δv=464 Hz), 32.96 (Δv=278 Hz), 23.16 (Δv=125 Hz), 16.43 (Δv=135 Hz), 7.37 (Δv=24 Hz), 7.26 (Δv=13 Hz), 7.12 (Δv=17 Hz), 6.98 (Δv=18 Hz), 6.86 (Δv=13 Hz), 6.68 (Δv=70 Hz), 2.49 (Δv=84 Hz), 2.32 (Δv=15 Hz), 2.19 (Δv= 20 Hz), 1.50 (Δv=9 Hz), 1.09 (Δv=120 Hz), 0.37 (Δv=49 Hz), -11.66 (Δv=70 Hz), -12.44 (Δv=55 Hz), -15.71 (s), -20.28 (s), -36.11 (Δv=869 Hz), -55.80 (Δv=201 Hz).

	(18)	(17)	(19)
Formula	$C_{67}H_{79}Br_2Mn_2N_2$	$C_{67}H_{79}Br_2Co_2N_2$	$C_{31}H_{34}ClZnN$
Temperature (K)	122	120	120
M_w	1110.92	1118.91	521.45
Crystal system	Monoclinic	Monoclinic	Monoclinic
Space Group	P2/n	P2/n	$P2_1/n$
a (Å)	14.1860(14)	14.0013(2)	8.5851(4)
b (Å)	12.304(2)	12.2213(2)	26.0439(12)
c (Å)	17.118(2)	17.0964(2)	11.9486(7)
α (°)	90	90	90
β *(°)*	90.085(12)	91.0870(10)	97.735(5)
γ *(°)*	90	90	90
V *($Å^3$)*	2987.9(7)	2924.91(7)	2647.3(2)
Z'	0.5	0.5	1
R_1 (%)	16.25	2.30	10.41
wR_2 (%)	49.56	6.12	32.70
Crystal dimensions (mm^3)	0.079 x 0.068 x 0.063	0.076 x 0.127 x 329	0.697 x 0.152 x 0.103
2θ range (°)	7.13 to 150.53	7.23 to 149.29	6.78 to 146.53
Measured reflections	28967	73863	10883
R_{int}	0.4112	0.0341	0.0407
Unique reflections	5914	5972	5155
Completeness of data (%)	99.23	100	99.73

*Figure 2.4.2 Table of crystallographic data collected from the structures obtained (**17-19**). The Mn and Co complexes are isostructural and dimeric, in comparison to the monomeric Zn structure. This is most likely a consequence of the reduction seen in size across a period, though could also be due to the increased size of Br in comparison to Cl.*

5.6 Synthesis of Di-*Tert*-Butyl Pyridine Complexes:

[$Mes_2C_6H_3ZnCl$(2,6-di-*tert*-butylpyridine)] (22)

2,6-Di-*tert*-butylpyridine (6.44 µl, 0.029 mmol) was added to a solution of $[Mes_2C_6H_3ZnCl]_2.[LiCl(OEt_2)]_2$ (15 mg, 0.014 mmol) in C_6D_6 (0.6 ml). No colour change was observed and crystals have not yet been produced. Pictured below is the most likely product for the reaction.

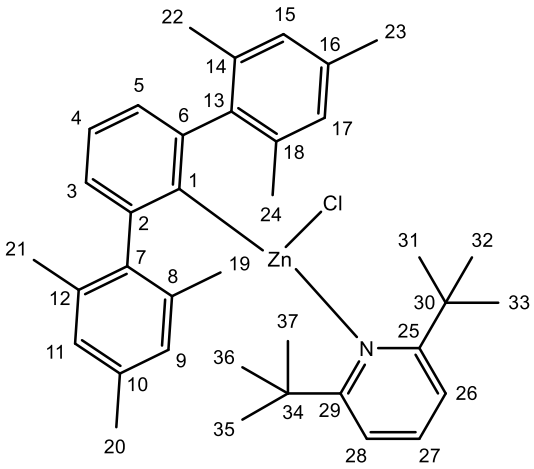

<u>^{1}H NMR (400MHz, C_6D_6, 298K): δ (ppm):</u> 7.21 (t, 1H, J=7.88 Hz, **(4)**), 7.01 (d, 2H, J=7.56 Hz, **(3, 5)**), 6.92 (d, 2H, J= 7.8 Hz, **(26, 28)**), 6.87 (t, 1H, J=5.24 Hz, **(27)**), 6.85 (s, 4H, **(9, 11, 15, 17)**), 2.22 (s, 6H, **(20,23)**), 2.08 (s, 12H, **(19,21,22,24)**), 1.40 (s, 18H, **(31,32,33,35,36,37)**).

<u>^{13}C NMR (400MHz, C_6D_6, 298K): δ (ppm):</u> 167.47, 149.6, 147.63, 143.09, 142.22, 141.62, 139.13, 136.86, 136.09, 136.02 **(4)**, 135.71, 135.42, 135.02, 130.36, 128.74, 128.52, 128.31 **(9,11, 15,17)**, 128.15 **(27)**, 127.37 **(3,5)**, 125.64 **(3,5)**, 115.36, 37.44, 30.03 **(31, 32, 33, 34, 35, 36, 37)**, 26.88, 20.63, 20.15,

[$Mes_2C_6H_3CoBr$(2,6-di-*tert*-butylpyridine)] (23)

2,6-Di-*tert*-butylpyridine (7.16 µl, 0.032 mmol) was added to a solution of $[Mes_2C_6H_3CoBr]_2.[LiBr(OEt_2)]_2$ (20 mg, 0.016 mmol) in C_6D_6 (0.6 ml). Colour change was observed from a deep green to a dark brown green. Pictured below is two possible products for the reaction.

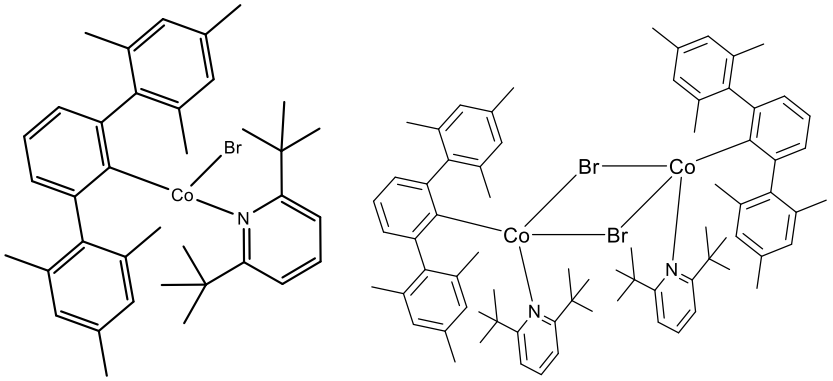

^{1}H NMR (400MHz, C_6D_6, 298K): δ (ppm) (all peaks appear as singlets): 22.76 (Δv=32 Hz), 7.28 (Δv=23 Hz), 7.14 (s), 6.99 (Δv=21 Hz), 6.90 (s), 5.49 (Δv=71 Hz), 2.58 (Δv=55 Hz), 2.33 (Δv=16 Hz), 2.20 (Δv=20 Hz), 1.52 (Δv=14 Hz), 0.43 (Δv=16 Hz), -3.48 (Δv=28 Hz), -10.55 (Δv=35 Hz), -11.49 (Δv=62 Hz).

[$Mes_2C_6H_3FeCl$(2,6-di-*tert*-butylpyridine)] (24)

2,6-Di-*tert*-butylpyridine (8.62 µl, 0.038 mmol) was added to a solution of $[Mes_2C_6H_3FeCl]_2.[LiCl(OEt_2)]_2$ (20 mg, 0.019 mmol) in C_6D_6 (0.6 ml). No colour change was observed and crystals have not yet been produced.

^{1}H NMR (400MHz, C_6D_6, 298K): δ (ppm) (all peaks appear as singlets): 31.44 (Δv=236 Hz), 7.27 (Δv=27 Hz), 7.12 (s), 6.99 (Δv=40 Hz), 6.88 (s), 2.33 (Δv=36 Hz), 2.19 (Δv=29 Hz), 1.50 (Δv=21 Hz), 0.40 (Δv=33 Hz), -11.15 (Δv=57 Hz), -34.88 (Δv=977 Hz), -53.93 (Δv=253 Hz).

[$Mes_2C_6H_3MnBr$(2,6-di-*tert*-butylpyridine)] (25)

2,6-Di-*tert*-butylpyridine (7.29 µl, 0.0325 mmol) was added to a solution of $[Mes_2C_6H_3MnBr]_2.[LiBr(OEt_2)]_2$ (20 mg, 0.016 mmol) in C_6D_6 (0.6 ml). No colour change was observed. Pictured below is two possible products for the reaction.

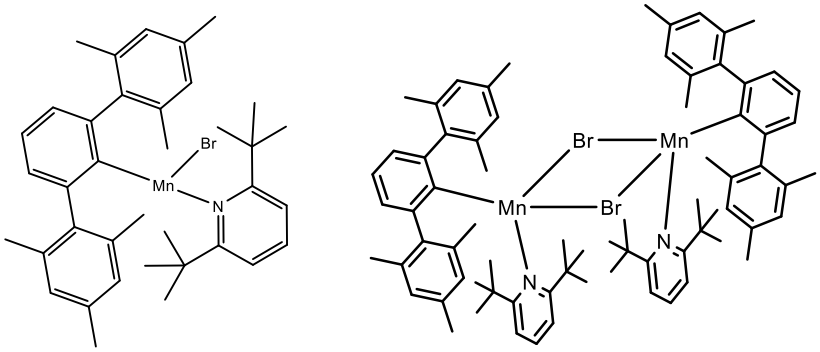

^{1}H NMR (400MHz, C_6D_6, 298K): δ (ppm) (all peaks appear as singlets): 11.80 (Δv=398 Hz), 7.27 (Δv=32 Hz), 7.11 (Δv=38 Hz), 6.99 (Δv=49 Hz), 2.33 (Δv=45 Hz), 2.18 (Δv=40 Hz), 1.51 (Δv=27 Hz), 0.40 (Δv=37 Hz).

6. References

1 R. Poli, *Chem. Rev.*, 1996, **96**, 2135–2204.

2 R. H. Crabtree, *The Organometallic Chemistry Of The Transition Metals*, WILEY, Fifth Edit., 2009.

3 W. Pope and S. Peachey, *J. Chem. Soc. Trans.*, 1909, **95**, 571–576.

4 J. S. Thayer, *J. Chem. Educ.*, 1969, **46**, 442.

5 T. L. Davis, *J. Chem. Educ.*, 1929, **6**, 1403.

6 M. Hancock and J. Ariyoshi, *Angew. Chem. Int. Ed.*, 1969, **8**, 410–420.

7 P. E. M. Siegbahn, *J. Phys. Chem.*, 1995, **99**, 12723–12729.

8 P. O. Stoutland, R. G. Bergman, S. P. Nolan and C. D. Hoff, *Polyhedron*, 1988, **7**, 1429–1440.

9 A. Shortland, G. Yagupsky, N. J. Hill, M. Yagupsky and G. Wilkinson, *J. Chem. Soc., Dalton Trans.*, 1972, 533–542.

10 J. Vela, S. Vaddadi, T. R. Cundari, J. M. Smith, E. A. Gregory, R. J. Lachicotte, C. J. Flaschenriem and P. L. Holland, *Organometallics*, 2004, **23**, 5226–5239.

11 R. P. A. Sneeden and H. H. Zeiss, *J. Organomet. Chem.*, 1970, **22**, 713–722.

12 H. Clavier and S. P. Nolan, *Chem. Commun.*, 2010, **46**, 841–861.

13 B. A. J. Shortland and G. Wilkinson, *J. Chem. Soc., Dalton Trans.*, 1973, 872–876.

14 V. Pfennig and K. Seppelt, *Science.*, 1996, **271**, 626–628.

15 B. S. E. Binns, R. H. Cragg, R. D. Gillard, F. Pilbrow, C. F. H. Tipper, D. M. Adams, J. Chatt, R. G. Guy, N. Sheppard, D. M. Adams, J. Chatt, R. G. Guy and M. Keeton, *J. Chem. Soc. A*, 1969, 1227–1231.

16 A. Bakac, J. A. Janni and J. H. Espenson, *Inorg. Chem.*, 1992, **31**, 1088–1090.

17 E. Frankland, *Q. J. Chem. Soc.,* 1850, **2**, 263–296.

18 J. Bacsa, F. Hanke, S. Hindley, R. Odedra, G. R. Darling, A. C. Jones and A. Steiner, *Angew. Chemie - Int. Ed.*, 2011, **50**, 11685–11687.

19 I. Kondolff, H. Doucet and M. Santelli, *Organometallics*, 2006, **25**, 5219–5222.

20 Y. Tamaru, A. Tanaka, K. Yasui, S. Goto and S. Tanaka, *Angew. Chemie Int. Ed. English*, 1995, **34**, 787–789.

21 K. Maruyama and T. Katagiri, *J. Phys. Org. Chem.*, 1989, **2**, 205–213.

22 W. Kaminsky, *Dalton Trans.,* 1998, 1413–1418.

23 G. Wilkinson, M. Rosenblum, M. . Whiting and R. . Woodward, *J. Am. Chem. Soc.*, 1952, **74**, 2125–2126.

24 J. D. Dunitz, L. E. Orgel and A. Rich, *Acta Cryst.*, 1956, **9**, 373–375.

25 R. H. Grubbs, *Olefin Metathesis Catalysts for the Preparation of Molecules and Materials*, 2005.

26 R. R. Schrock, *Multiple Metal-Carbon Bonds for Catalytic Metathesis Reactions*, 2005.

27 Y. Chauvin, *Olefin Metathesis: The Early Days*, 2005.

28 R. F. Heck, *Palladium Reactions for Organic Syntheses*, 2010.

29 E. Negishi, *Magical Power of Transition Metals: Past, Present, and Future*, 2010.

30 A. Suzuki, *Cross-coupling Reactions of Organoboranes: An Easy Way for C-C Bonding*, 2010.

31 N. H. Buttrus, C. Eaborn, P. B. Hitchcock, J. D. Smith and A. C. Sullivan, *J. Chem. Soc., Chem. Commun*, 1985, 1380–1381.

32 A. A. Danopoulos, P. Braunstein, K. Y. Monakhov, J. Van Leusen, P. Kögerler, M. Clémancey, J. M. Latour, A. Benayad, M. Tromp, E. Rezabal and G. Frison, *Dalton Trans.,* 2017, **46**, 1163–1171.

33 P. P. Power, *Chem. Rev.*, 2012, 112, 3482–3507.

34 D. L. Kays, *Organomet. Chem.*, 2010, **36**, 56–76.

35 A. D. Sutton, T. Ngyuen, J. C. Fettinger, M. M. Olmstead, G. J. Long and P. P. Power, *Inorg. Chem.*, 2007, **46**, 4809–4814.

36 D. L. Kays and A. R. Cowley, *Chem. Commun.*, 2007, 1053–1055.

37 H. R. Sharpe, A. M. Geer, L. J. Taylor, B. M. Gridley, T. J. Blundell, A. J. Blake, E. S. Davies, W. Lewis, J. McMaster, D. Robinson and D. L. Kays, *Nat. Commun.*, 2018, **9**, 3757.

38 H. R. Sharpe, A. M. Geer, T. J. Blundell, F. R. Hastings, M. W. Fay, G. A. Rance, W. Lewis, A. J. Blake and D. L. Kays, *Catal. Sci. Technol.*, 2018, **8**, 229–235.

39 H. R. Sharpe, A. M. Geer, H. E. L. Williams, T. J. Blundell, W. Lewis, A. J. Blake and D. L. Kays, *Chem. Commun.*, 2017, **53**, 937–940.

40 C. Ni, H. Lei and P. P. Power, *Organometallics*, 2010, **29**, 1988–1991.

41 C. Ni and P. P. Power, *Chem. Commun.*, 2009, 5543–5545.

42 N. Tailuan, A. D. Sutton, 1 Marcin Brynda, J. C. Fettinger, G. J. Long and P. P. Power, *Science.*, 2005, **310**, 844–848.

43 M. Brynda, L. Gagliardi, P. O. Widmark, P. P. Power and B. O. Roos, *Angew. Chemie - Int. Ed.*, 2006, **45**, 3804–3807.

44 R. Fischer, H. Görls, M. Friedrich and M. Westerhausen, *J. Organomet. Chem.*, 2009, **694**, 1107–1111.

45 S. S. Lau, P. E. Fanwick and A. Walton, *Polyhedron*, 1997, **16**, 3649–3654.

46 R. Wolf, C. Ni, T. Nguyen, M. Brynda, G. J. Long, A. D. Sutton, R. C. Fischer, J. C. Fettinger, M. Hellman, L. Pu and P. P. Power, *Inorg. Chem.*, 2007, **46**, 11277–11290.

47 C. Ni, B. D. Ellis, J. C. Fettinger, G. J. Long and P. P. Power, *Chem. Commun.*, 2008, 1014–1016.

48 R. Wolf, M. Brynda, C. Ni, G. J. Long and P. P. Power, *J. Am. Chem. Soc.*, 2007, **129**, 6076–6077.

49 A. Saednya and H. Hart, *Synthesis (Stuttg).*, 1996, 1455–1458.

50 K. Ruhlandt-Senge, J. J. Ellison, R. J. Wehmschulte, F. Pauer and P. P. Power, *J. Am. Chem. Soc.*, 1993, **115**, 11353–11357.

51 J. J. Ellison and P. P. Power, *J. Organomet. Chem.*, 1996, **526**, 263–267.

52 D. L. Kays, *Dalton Trans.,* 2011, 40, 769–778.

53 H. R. Sharpe, A. M. Geer, W. Lewis, A. J. Blake and D. L. Kays, *Angew. Chemie - Int. Ed.*, 2017, **56**, 4845–4848.

54 Y. Sun, Z. Zhang, X. Wang, X. Li and X. Zhou, *Dalton Trans.,* 2010, **39**, 221–226.

55 Y. Sun, Z. Zhang, X. Wang, X. Li, L. Weng and X. Zhou, *Dalton Trans.,* 2010, **39**, 221–226.

56 P. Štěpnika, *Chem. Soc. Rev.*, 2012, **41**, 4273–4305.

57 D. Benito-garagorri, I. Lagoja, F. Veiros, K. A. Kirchner and D. Benito-garagorri, *Dalton Trans.,* 2011, **40**, 4778–4792.

58 Z. Mo and L. Deng, *Coord. Chem. Rev.*, 2017, 1–15.

59 A. A. Danopoulos, P. Braunstein, N. Stylianides and M. Wesolek, *Organometallics*, 2011, **30**, 6514–6517.

60 C. R. Ganivet, B. Ballesteros, G. De La Torre, J. M. Clemente-Juan, E. Coronado and T. Torres, *Chem. - A Eur. J.*, 2013, **19**, 1457–1465.

61 D. Gatteschi, R. Sessoli and A. Cornia, *Chem. Commun.*, 2000, 725–732.

62 M. I. Lipschutz, T. Chantarojsiri, Y. Dong, T. D. Tilley, M. I. Lipschutz, T. Chantarojsiri, Y. Dong and T. D. Tilley, *J. Am. Chem. Soc.*, 2015, **137**, 6366–6372.

63 C. Ni, T. A. Stich, J. Long and P. P. Power, *Chem. Commun.*, 2010, **46**, 4466–4468.

64 E. O. Fischer and A. Maasbol, *Chem. Commun.*, 1964, **3**, 3–4.

65 A. J. Arduengo and G. Bertrand, *Chem. Rev.*, 2009, **109**, 3209–3210.

66 D. J. Cardin, B. Cetinkaya and M. F. Lappert, *Chem. Rev.*, 1972, **72**, 545–574.

67 M. N. Hopkinson, C. Richter, M. Schedler and F. Glorius, *Nature*, 2014, **510**, 485–496.

68 P. Schwab, R. H. Grubbs, J. W. Ziller and R. V August, *J. Am. Chem. Soc.*, 1996, **118**, 100–110.

69 C. A. Richards, S. Kim, Y. Yamaguchi and H. F. S. Iii, *J. Am. Chem. Soc.*, 1995, **117**, 10104–10107.

70 K. Hirai, T. Itoh and H. Tomioka, *Chem. Rev.*, 2009, **109**, 3275–3332.

71 R. R. Schrock, *J. Am. Chem. Soc.*, 1974, **96**, 6796–6797.

72 R. R. Schrock, *Chem. Rev.*, 2002, **102**, 145–179.

73 M. Brookhart, M. L. H. Green and G. Parkin, *Proc. Natl. Acad. Sci.*, 2007, **104**, 6908–6914.

74 R. R. Schrock and C. Cope, *Organometallics*, 2017, **36**, 1884–1892.

75 E. Despagnet-Ayoub and R. H. Grubbs, *J. Am. Chem. Soc.*, 2004, **126**, 10198–10199.

76 S. Würtemberger-pietsch, U. Radius, T. B. Marder, S. Würtemberger-pietsch and S. Würtemberger-, *Dalton Trans.,* 2016, **45**, 5880–5895.

77 D. J. D. Wilson and J. L. Dutton, *Dalton Trans.,* 2014, **43**, 12807–13146.

78 A. Poater, F. Ragone, S. Giudice, C. Costabile, R. Dorta, S. P. Nolan, L. Cavallo, D. Chimica and V. Uni, *Organomet. Chem.*, 2008, **27**, 2679–2681.

79 A. J. Arduengo and M. Kline, *J. Am. Chem. Soc.*, 1991, **113**, 361–363.

80 R. Hoffmann, R. Gleiter and F. B. Mallory, *J. Am. Chem. Soc.*, 1970, **92**, 1460–1466.

81 R. W. Alder, M. E. Blake, L. Chaker, J. N. Harvey, F. Paolini and J. Schütz, *Angew. Chemie - Int. Ed.*, 2004, **43**, 5896–5911.

82 A. C. Hillier, W. J. Sommer, B. S. Yong, J. L. Petersen, L. Cavallo and S. P. Nolan, *Organometallics*, 2003, **22**, 4322–4326.

83 C. A. Tolman, *Chem. Rev.*, 1976, **77**, 313–348.

84 A. Poater, B. Cosenza, A. Correa, S. Giudice, F. Ragone, V. Scarano and L. Cavallo, *Eur. J. Inorg. Chem.*, 2009, 1759–1766.

85 G. Ciancaleoni, N. Scafuri, G. Bistoni, A. Macchioni, F. Tarantelli, D. Zuccaccia and L. Belpassi, *Inorg. Chem.*, 2014, **53**, 9907–9916.

86 E. Peris and R. H. Crabtree, *Coord. Chem. Rev.*, 2004, **248**, 2239–2246.

87 M. Beller, G. C. Fortman and S. P. Nolan, *Chem. Soc. Rev.*, 2011, **40**, 5151–5169.

88 T. Weskamp, W. C. Schattenmann, M. Spiegler and W. A. Herrmann, *Angew. Chemie - Int. Ed.*, 1998, **37**, 2490–2493.

89 D. Bøzier, G. T. Venkanna, J. Sortais and C. Darcel, *ChemCatChem*, 2011, **3**, 1747–1750.

90 P. D. Stevens, G. Li, J. Fan, M. Yen and Y. Gao, *Chem. Commun.*, 2005, 4435–4437.

91 V. Lavallo, Y. Canac, C. Präsang, B. Donnadieu and G. Bertrand, *Angew. Chemie - Int. Ed.*, 2005, **44**, 5705–5709.

92 M. Melaimi, R. Jazzar, M. Soleilhavoup and G. Bertrand, *Angew. Chemie - Int. Ed.*, 2017, **56**, 10046–10068.

93 O. Back, M. Henry-ellinger, C. D. Martin, D. Martin and G. Bertrand, *Angew.*

Chemie - Int. Ed., 2013, **52**, 2939–2943.

94 M. Soleilhavoup and G. Bertrand, *Acc. Chem. Res.*, 2015, **48**, 256–266.

95 P. P. Samuel, K. C. Mondal, N. A. Sk, H. W. Roesky, E. Carl, R. Neufeld, D. Stalke, S. Demeshko, F. Meyer, L. Ungur, L. F. Chibotaru, J. Christian, V. Ramachandran, J. Van Tol and N. S. Dalal, *J. Am. Chem. Soc.*, 2014, **136**, 11964–11971.

96 P. P. Samuel, R. Neufeld, K. Chandra Mondal, H. W. Roesky, R. Herbst-Irmer, D. Stalke, S. Demeshko, F. Meyer, V. C. Rojisha, S. De, P. Parameswaran, A. C. Stückl, W. Kaim, J. H. Christian, J. K. Bindra and N. S. Dalal, *Chem. Sci.*, 2015, **6**, 3148–3153.

97 K. C. Mondal, S. Roy, S. De, P. Parameswaran, B. Dittrich, F. Ehret, W. Kaim and H. W. Roesky, *Chem. - A Eur. J.*, 2014, **20**, 11646–11649.

98 H. Zhang, Z. Ouyang, Y. Liu, Q. Zhang, L. Wang and L. Deng, *Angew. Chemie - Int. Ed.*, 2014, **53**, 8432–8436.

99 D. R. Anderson, V. Lavallo, D. J. O'Leary, G. Bertrand and R. H. Grubbs, *Angew. Chemie - Int. Ed.*, 2007, **46**, 7262–7265.

100 D. R. Anderson, T. Ung, G. Mkrtumyan, G. Bertrand, R. H. Grubbs and Y. Schrodi, *Organometallics*, 2008, **27**, 563–566.

101 X. Zeng, G. D. Frey, R. Kinjo, B. Donnadieu and G. Bertrand, *J. Am. Chem. Soc.*, 2009, **131**, 8690–8696.

102 S. Roy, K. C. Mondal and H. W. Roesky, *Acc. Chem. Res.*, 2016, **49**, 357–369.

103 B. V Popp and S. S. Stahl, *Chem. - A Eur. J.*, 2009, **15**, 2915–2922.

104 C. Bianchini, G. Giambastiani, L. Luconi and A. Meli, *Coord. Chem. Rev.*, 2010, **254**, 431–455.

105 V. C. Gibson, C. Redshaw and G. A. Solan, *Chem. Rev.*, 2007, **107**, 1745–1776.

106 C. Y. Lin, J. C. Fettinger and P. P. Power, *Inorg. Chem.*, 2017, **56**, 9892–9902.

107 P. L. Holland, *Acc. Chem. Res.*, 2015, **48**, 1696–1702.

108 R. Jazzar, J. B. Bourg, R. D. Dewhurst, B. Donnadieu and G. Bertrand, *J. Org. Chem.*, 2007, **72**, 3492–3499.

109 J. Clayden, N. Greeves, S. Warren and P. Wothers, *Organic Chemistry*, Oxford University Press, 1st Editio., 2001.

110 R. W. Layer, *Chem. Rev.*, 1963, **63**, 489–510.

111 Z. Zhu, M. Brynda, R. J. Wright, R. C. Fischer, W. A. Merrill, E. Rivard, R. Wolf, J. C. Fettinger, M. M. Olmstead and P. P. Power, *J. Am. Chem. Soc.*, 2007, **129**, 10847–10857.

112 C. Ni, J. C. Fettinger, G. J. Long and P. P. Power, *Dalton Trans.,* 2010, **39**, 10664–10670.

113 R. D. Shannon, *Acta Cryst.*, 1976, **32**, 751–767.

114 P. Thuéry, H. Lee and J. Harrow, *Dalton Trans.,* 2014, **43**, 5662–5666.

115 W. B. Jennings, B. M. Farrell and J. F. Malone, *Acc. Chem. Res.*, 2001, **34**, 885–894.

116 Y. Umezawa, S. Tsuboyama and M. Nishiot, *Tetrahedron*, 1999, **55**, 10047–10056.

117 J. Hicks and C. Jones, *Inorg. Chem.*, 2013, **52**, 3900–3907.

118 R. F. See, R. A. Kruse and W. M. Strub, *Inorg. Chem.*, 1998, **37**, 5369–5375.

119 D. F. Evans, *J. Chem. Soc.*, 1959, 2003–2005.

120 D. Basumatary, R. Ashray and A. Kumar, *J. Mol. Struct.*, 2015, **1092**, 122–129.

121 D. Ostfeld and I. A. Cohen, *J. Chem. Educ.*, 1972, **49**, 829.

122 B. J. Cosier and A. M. Glazer, *J. Appl. Crystallogr.*, 1986, **19**, 105–107.

123 O. V. Dolomanov, L. J. Bourhis, R. J. Gildea, J. A. K. Howard and H. Puschmann, *J. Appl. Crystallogr.*, 2009, **42**, 339–341.

124 G. M. Sheldrick, *Acta Crystallogr. Sect. C Struct. Chem.*, 2015, **71**, 3–8.

125 J. E. Borger, A. W. Ehlers, M. Lutz, J. C. Slootweg and K. Lammertsma, *Angew. Chemie - Int. Ed.*, 2014, **53**, 12836–12839.